AN ASYMPTOTIC ANALYSIS OF THE MEAN FIRST PASSAGE TIME FOR NARROW ESCAPE PROBLEMS: PART I: TWO-DIMENSIONAL DOMAINS[*]

S. PILLAY[†], M. J. WARD[†], A. PEIRCE[†], AND T. KOLOKOLNIKOV[‡]

Abstract. The mean first passage time (MFPT) is calculated for a Brownian particle in a bounded two-dimensional domain that contains N small nonoverlapping absorbing windows on its boundary. The reciprocal of the MFPT of this narrow escape problem has wide applications in cellular biology, where it may be used as an effective first-order rate constant to describe, for example, the nuclear export of messenger RNA molecules through nuclear pores. In the asymptotic limit where the absorbing patches have small measure, the method of matched asymptotic expansions is used to calculate the MFPT in an arbitrary two-dimensional domain with a smooth boundary. The theory is extended to treat the case where the boundary of the domain is piecewise smooth. The asymptotic results for the MFPT depend on the surface Neumann Green's function of the corresponding domain and its associated regular part. The known analytical formulae for the surface Neumann Green's function for the unit disk and the unit square provide explicit asymptotic approximations to the MFPT for these special domains. For an arbitrary two-dimensional domain with a smooth boundary, the asymptotic MFPT is evaluated by developing a novel boundary integral method to numerically calculate the required surface Neumann Green's function.

Key words. narrow escape, mean first passage time, matched asymptotic expansions, logarithmic expansions, surface Neumann Green's functions

AMS subject classifications. 35B25, 35C20, 35P15, 35J05, 35J08

DOI. 10.1137/090752511

1. Introduction. Narrow escape problems have recently gained increasing scientific interest (cf. [1], [9], [10], [17]), especially in biological modeling, since they arise naturally in the description of Brownian particles that attempt to escape from a bounded domain through small absorbing windows on an otherwise reflecting boundary. In the biological context, the Brownian particles could be diffusing ions, globular proteins, or cell-surface receptors. It is then of interest to determine, for example, the mean time that an ion requires to find an open ion channel located in the cell membrane or the mean time of a receptor to hit a certain target binding site (cf. [10], [17]).

The narrow escape problem in a two-dimensional domain is described as the motion of a Brownian particle confined in a bounded domain $\Omega \in R^2$ whose boundary $\partial\Omega = \partial\Omega_r \cup \partial\Omega_a$ is almost entirely reflecting ($\partial\Omega_r$), except for small absorbing windows, labeled collectively by $\partial\Omega_a$, through which the particle can escape (see Figure 1). Denoting the trajectory of the Brownian particle by $X(t)$, the mean first passage time (MFPT) $v(x)$ is defined as the expectation value of the time τ taken for the Brownian particle to become absorbed somewhere in $\partial\Omega_a$ starting initially from $X(0) = x \in \Omega$, so that $v(x) = E[\tau \mid X(0) = x]$. The calculation of $v(x)$ becomes a narrow escape

problem in the limit when the measure of the absorbing set $|\partial\Omega_a| = \mathcal{O}(\varepsilon)$ is asymptotically small, where $0 < \varepsilon \ll 1$ measures the dimensionless radius of an absorbing window.

It is well known (cf. [10], [15], [16]) that the MFPT $v(x)$ satisfies a Poisson equation with mixed Dirichlet–Neumann boundary conditions, formulated as

$$(1.1a) \qquad \triangle v = -\frac{1}{D}, \quad x \in \Omega,$$

$$(1.1b) \quad v = 0, \qquad x \in \partial\Omega_a = \bigcup_{j=1}^{N} \partial\Omega_{\varepsilon_j}, \quad j = 1, \ldots, N; \qquad \partial_n v = 0, \qquad x \in \partial\Omega_r,$$

where D is the diffusion coefficient associated with the underlying Brownian motion. In (1.1), the absorbing set consists of N small disjoint absorbing windows $\partial\Omega_{\varepsilon_j}$ centered at $x_j \in \partial\Omega$ (see Figure 1). In our two-dimensional setting, we assume that the length of each absorbing arc is $|\partial\Omega| = \varepsilon l_j$, where $l_j = \mathcal{O}(1)$. It is further assumed that the windows are well separated in the sense that $|x_i - x_j| = \mathcal{O}(1)$ for all $i \neq j$. With respect to a uniform distribution of initial points $x \in \Omega$, the average MFPT, denoted by $\bar{v}$, is defined by

$$(1.2) \qquad \bar{v} = \chi \equiv \frac{1}{|\Omega|} \int_{\Omega} v(x) \, dx,$$

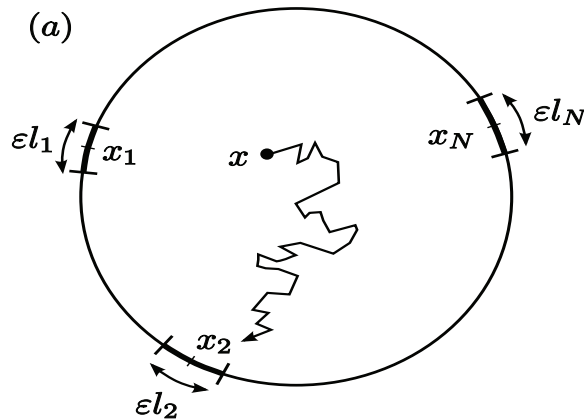where $|\Omega|$ denotes the area of Ω.

FIG. 1. *Sketch of a Brownian trajectory in the two-dimensional unit disk with absorbing windows on the boundary.*

Since the MFPT diverges as $\varepsilon \to 0$, the calculation of the MFPT $v(x)$, and that of the average MFPT $\bar{v}$, constitutes a singular perturbation problem. It is the goal of this paper to systematically use the method of matched asymptotic expansions to extend previous results on two-dimensional narrow escape problems in three main directions: (i) to examine the effect on the MFPT of multiple absorbing windows on the boundary, (ii) to provide both a two-term and an infinite-order logarithmic asymptotic expansion for the solution v to (1.1) for arbitrary two-dimensional domains with a smooth boundary, and (iii) to develop and implement a numerical method to compute the surface Neumann Green's function, which is required for evaluating certain terms in the asymptotic results.

For a two-dimensional domain with a smooth boundary with one small window of length $\mathcal{O}(\varepsilon)$ on its boundary, the analysis in [10] and [18] showed that, for $\varepsilon \to 0$, $v(x)$ has the leading-order expansion

$$(1.3) \qquad v(x) = \frac{|\Omega|}{\pi D} \left[-\log \varepsilon + \mathcal{O}(1) \right].$$

This leading-order result is independent of x and the location of the window on $\partial\Omega$. A related leading-order asymptotic result for $v(x)$ was obtained in [19] for the case where an absorbing window is centered at a cusp or corner point of a nonsmooth boundary, and an explicit two-term result for this case was obtained for a rectangular domain. The $\mathcal{O}(1)$ term in (1.3), which depends on x and on the arrangements of the absorbing windows on the domain boundary, has been determined previously in only a few special situations. In particular, for the unit disk with one absorbing window on the boundary, the $\mathcal{O}(1)$ term in (1.3) was calculated explicitly in [18] by using the Collins method to solve certain dual integral equations. The only previous work on the interaction effect of multiple absorbing windows was given in [11] for the case of two absorbing windows on the boundary of the unit disk with either an $\mathcal{O}(1)$ or an $\mathcal{O}(\varepsilon)$ separation between the windows. For this two-window case, the result in [11] determined the average MFPT $\bar{v}$ up to an unspecified $\mathcal{O}(1)$ term, which was fit through Brownian particle numerical simulations.

One specific goal of this paper is to use the method of matched asymptotic expansions to derive an analytical expression for the $\mathcal{O}(1)$ term in (1.3) for an arbitrary domain with a smooth boundary that has N well-separated absorbing windows on the boundary. In addition, further terms in the asymptotic expansion of $v(x)$, of higher order than in (1.3), are obtained by summing a certain infinite-order logarithmic expansion. In our analysis, the average MFPT $\bar{v}$, defined in (1.2), is also readily calculated. Our asymptotic results for the MFPT involve, in a rather essential way, the surface Neumann Green's function for the Laplacian together with the regular part of this Green's function. Our asymptotic results for $v(x)$ in an arbitrary domain are given in Principal Results 2.1 and 2.2 and show clearly the nontrivial interaction effect of well-separated absorbing windows. We then show how our analysis is very easily adapted to treat the case where a finite number of nonoverlapping windows are clustered in an $\mathcal{O}(\varepsilon)$ neighborhood around some point on the domain boundary. Specializing to a two-window cluster on the unit disk, our result for this case agrees with that in [11] and determines analytically the missing $\mathcal{O}(1)$ term not given in [11].

In section 3, we implement and illustrate the analytical theory of section 2 for some specific domains. In subsections 3.1 and 3.2, simple analytical results for $v(x)$ and $\bar{v}$ are obtained for various arrangements of the small absorbing windows on the boundary of the unit disk and unit square. For such special domains, the surface Neumann Green's function can be determined analytically. For the case of one absorbing window on the boundary of the unit disk, our results readily reduce to those of [18]. For the case of N asymptotically small, equally spaced, windows of a common length 2ε on the boundary of the unit disk, our analysis for the average MFPT yields the explicit asymptotic result

$$(1.4) \qquad \bar{v} \sim \frac{1}{DN} \left[-\log\left(\frac{\varepsilon N}{2}\right) + \frac{N}{8} \right].$$

Other results for $v(x)$ and $\bar{v}$ are given in subsections 3.1 and 3.2. In subsection 3.2, we extend the analysis in section 2 to allow for an absorbing window at a corner of

the square, representing a nonsmooth point on $\partial\Omega$. Our result for this case agrees with that derived in [19]. In subsection 3.3, we develop and implement a novel boundary integral numerical scheme to numerically compute the surface Neumann Green's function and its regular part for an arbitrary bounded two-dimensional domain with a smooth boundary. The numerical method is then used to calculate $v(x)$ and $\bar{v}$ for an ellipse.

The problem for the MFPT is very closely related to the problem of determining the principal eigenvalue λ^* for the Laplacian in a domain where the reflecting boundary is perturbed by N asymptotically small absorbing windows of length $\mathcal{O}(\varepsilon)$. For a two-dimensional domain with a smooth boundary, in section 4 we show that

$$(1.5) \qquad \bar{v} = \chi = \frac{1}{D\lambda^*(\varepsilon)} + \mathcal{O}\left(|\mu|^2\right),$$

where $|\mu|^2$ indicates terms of order $\mathcal{O}\left[(-1/\log\varepsilon)^2\right]$. The specific order of this error estimate is a new result. In addition, the method of matched asymptotic expansions is used to obtain both a two-term and an infinite-order asymptotic result for λ^* in powers of $\mathcal{O}(-1/\log\varepsilon)$. These results for λ^* in Principal Results 4.1 and 4.2 extend the leading-order asymptotic theory of [23], where it was shown for the case of one absorbing window of length 2ε that $\lambda^* \sim \pi\mu/|\Omega|$, where $\mu = -1/\log(\varepsilon/2)$. Some related results for this problem, obtained using a different approach, are given in [7]. The analysis in section 4 is an extension of the work of [22] and [12] for the related problem of calculating a high-order asymptotic expansion for the principal eigenvalue of the Laplacian corresponding to a two-dimensional domain with a reflecting boundary that is punctured by N asymptotically small disks of a common radius ε.

For the case of one small absorbing arc of a fixed length εl_1 centered at $x_1 \in \partial\Omega$, the results of section 4 show that

$$(1.6) \qquad \lambda^* \sim \frac{\pi\mu_1}{|\Omega|} - \frac{\pi^2\mu_1^2}{|\Omega|}R(x_1;x_1) + \mathcal{O}(\mu_1^3), \qquad \mu_1 \equiv -\frac{1}{\log[\varepsilon d_1]}, \quad d_1 = \frac{l_1}{4},$$

where $R(x_1;x_1)$ is the regular part of the surface Neumann Green's function. In section 4, we seek to determine the location of the center $x_1 \in \partial\Omega$ of the absorbing arc that minimizes the second term for λ^* in (1.6) involving $R(x_1;x_1)$. For a heat conduction problem, this optimal absorbing arc is the one that minimizes the rate of heat loss across the domain boundary. Similar eigenvalue optimization problems have been studied in [8] and [3] as a function of the location of an absorbing boundary segment and in [12] for the related problem of asymptotically small disks that are interior to a two-dimensional domain. When Ω is a square it was proved in [3] that, for one small (but not asymptotically small) absorbing segment, the principal eigenvalue is minimized when this segment is centered at a corner of the square. Based on the results of [3] for the square it was conjectured in section 1 of [3] that, for a general convex domain with a smooth boundary, an optimal absorbing arc must lie in a region of $\partial\Omega$ with large curvature. This conjecture is investigated in section 4 by first deriving a perturbation result in Principal Result 4.3 for $R(x_1;x_1)$ for domains that are smooth perturbations of the unit disk. In Principal Result 4.4 we construct a counterexample to show that local minima of λ^* with respect to x_1 do not necessarily correspond to local maxima of the boundary curvature.

Related problems, with biophysical applications, involving the asymptotic calculation of either steady-state diffusion, Laplacian eigenvalues, or the MFPT, on specific Riemannian manifolds with a collection of localized traps, include [2] and [20] for the surface of a long cylinder and [4], [24], [19], and [6] for the surface of a sphere.

In Part II of this paper [5] we asymptotically calculate the MFPT for narrow escape from a spherical domain.

2. Narrow escape in two-dimensional domains. We construct the asymptotic solution to (1.1) in the limit $\varepsilon \to 0$ using the method of matched asymptotic expansions. The solution in the inner, or local, region near each absorbing arc is determined and then matched to an outer, or global, solution, valid away from $\mathcal{O}(\varepsilon)$ neighborhoods of each arc.

To construct the inner solution near the jth absorbing arc, we write (1.1) in terms of a local orthogonal coordinate system, where η denotes the distance from $\partial\Omega$ to $x \in \Omega$, and s denotes arclength on $\partial\Omega$. In terms of these coordinates, the problem (1.1a) for $v(x)$ transforms to the following problem for $w(\eta, s)$:

$$(2.1) \qquad \partial_{\eta\eta} w - \frac{\kappa}{1 - \kappa\eta} \partial_\eta w + \frac{1}{1 - \kappa\eta} \partial_s \left(\frac{1}{1 - \kappa\eta} \partial_s w \right) = -\frac{1}{D} \,.$$

Here κ is the curvature of $\partial\Omega$ and the center $x_j \in \partial\Omega$ of the jth absorbing arc transforms to $s = s_j$ and $\eta = 0$.

Next, we introduce the local variables $\hat{\eta} = \eta/\varepsilon$ and $\hat{s} = (s - s_j)/\varepsilon$ near the jth absorbing arc. Then, from (2.1) and (1.1b), we neglect $\mathcal{O}(\varepsilon)$ terms to obtain the inner problem

$$(2.2a) \qquad w_{0\hat{\eta}\hat{\eta}} + w_{0\hat{s}\hat{s}} = 0\,, \qquad 0 < \hat{\eta} < \infty\,, \quad -\infty < \hat{s} < \infty\,,$$
$$(2.2b) \qquad \partial_{\hat{\eta}} w_0 = 0 \quad \text{on } |\hat{s}| > l_j/2\,, \quad \hat{\eta} = 0\,; \qquad w_0 = 0 \quad \text{on } |\hat{s}| < l_j/2\,, \quad \hat{\eta} = 0\,.$$

We specify that w_0 has logarithmic growth at infinity, i.e., $w_0 \sim A_j \log |y|$ as $|y| \to \infty$, where A_j is an arbitrary constant and $|y| \equiv \varepsilon^{-1}|x - x_j| = \left(\hat{\eta}^2 + \hat{s}^2 \right)^{1/2}$. The solution w_0, unique up to the constant A_j, is readily calculated by introducing elliptic cylinder coordinates in (2.2). It has the far-field behavior

$$(2.3) \qquad w_0 \sim A_j \left[\log |y| - \log d_j + o(1) \right] \quad \text{as} \quad |y| \to \infty\,, \qquad d_j = l_j/4\,.$$

From the divergence theorem, $A_j = 2\pi^{-1} \int_0^{l_j/2} \partial_{\hat{\eta}} w_0|_{\hat{\eta}=0}\, ds$, which gives the flux of w_0 across the jth absorbing arc.

In the outer region, the jth absorbing arc shrinks to the point $x_j \in \partial\Omega$ as $\varepsilon \to 0$. With regards to the outer solution, the influence of each absorbing arc is, in effect, determined by a certain singularity behavior at each x_j that results from the asymptotic matching of the outer solution to the far-field behavior (2.3) of the inner solution. In this way, we obtain that the outer solution for v satisfies

$$(2.4a) \qquad \triangle v = -\frac{1}{D}\,, \qquad x \in \Omega\,; \qquad \partial_n v = 0\,, \qquad x \in \partial\Omega \backslash \{x_1, \ldots, x_N\}\,,$$

$$v \sim \frac{A_j}{\mu_j} + A_j \log |x - x_j| \quad \text{as} \quad x \to x_j\,, \quad j = 1, \ldots, N\,;$$

$$(2.4b)$$

$$\mu_j \equiv -\frac{1}{\log(\varepsilon d_j)}\,, \qquad d_j = \frac{l_j}{4}\,.$$

Each singularity behavior in (2.4b) specifies both the regular and the singular part of a Coulomb singularity. As such, it provides one constraint for the determination of a linear system for the source strengths A_j for $j = 1, \ldots, N$.

To solve (2.4), we introduce the surface Green's function $G(x; x_j)$ defined as the unique solution of

$$(2.5a) \qquad \triangle G = \frac{1}{|\Omega|}, \qquad x \in \Omega; \qquad \partial_n G = 0, \qquad x \in \partial\Omega \backslash \{x_j\},$$

$$(2.5b) \qquad G(x; x_j) \sim -\frac{1}{\pi} \log|x - x_j| + R(x_j; x_j) \quad \text{as } x \to x_j \in \partial\Omega,$$

$$(2.5c) \qquad \int_\Omega G(x; x_j)\, dx = 0,$$

where $|\Omega|$ is the area of Ω. Then, the solution to (2.4) is written in terms of $G(x; x_j)$ and an unknown constant χ, denoting the spatial average of v, by

$$(2.6) \qquad v = -\pi \sum_{i=1}^N A_i G(x; x_i) + \chi, \qquad \chi = \bar{v} \equiv \frac{1}{|\Omega|} \int_\Omega v\, dx.$$

To determine a linear algebraic system for A_j, for $j = 1, \ldots, N$, and for χ, we expand (2.6) as $x \to x_j$ and compare it with the required singularity behavior (2.4b). This yields that
(2.7)
$$A_j \log|x - x_j| - \pi A_j R_j - \pi \sum_{\substack{i=1 \\ i \neq j}}^N A_i G_{ji} + \chi = A_j \log|x - x_j| + \frac{A_j}{\mu_j}, \qquad j = 1, \ldots, N.$$

Here $G_{ji} \equiv G(x_j; x_i)$, while $R_j \equiv R(x_j; x_j)$ is the regular part of G given in (2.5b) at $x = x_j$. Equation (2.7) yields N linear equations for χ and A_j for $j = 1, \ldots, N$. We get the remaining equation by noting that $\triangle v = -\pi \sum_{i=1}^N A_i \triangle G = -\pi |\Omega|^{-1} \sum_{i=1}^N A_i = -D^{-1}$. Thus, the $N + 1$ constants χ and A_j, for $j = 1, \ldots, N$, satisfy

$$(2.8) \qquad \frac{A_j}{\mu_j} + \pi A_j R_j + \pi \sum_{\substack{i=1 \\ i \neq j}}^N A_i G_{ji} = \chi, \qquad j = 1, \ldots, N; \qquad \sum_{i=1}^N A_i = \frac{|\Omega|}{D\pi}.$$

This linear system of $N + 1$ equations can be written in matrix form as

$$(2.9) \qquad (I + \pi \mathcal{U}\mathcal{G})\mathcal{A} = \chi \mathcal{U}e, \qquad e^T \mathcal{A} = \frac{|\Omega|}{D\pi}.$$

Here $e^T \equiv (1, \ldots, 1)$, $\mathcal{A}^T \equiv (A_1, \ldots, A_N)$, and I is the $N \times N$ identity matrix, while the diagonal matrix $\mathcal{U}$ and symmetric Green's function matrix $\mathcal{G}$ are defined by

$$(2.10) \quad \mathcal{U} \equiv \begin{pmatrix} \mu_1 & 0 & \cdots & 0 \\ 0 & \ddots & \cdots & 0 \\ \vdots & \vdots & \ddots & \vdots \\ 0 & 0 & \cdots & \mu_N \end{pmatrix}, \qquad \mathcal{G} \equiv \begin{pmatrix} R_1 & G_{12} & \cdots & G_{1N} \\ G_{21} & R_2 & \cdots & G_{2N} \\ \vdots & \vdots & \ddots & \vdots \\ G_{N1} & \cdots & G_{N,N-1} & R_N \end{pmatrix}.$$

We can then decouple $\mathcal{A}$ and χ in (2.9) to obtain the following main result.

PRINCIPAL RESULT 2.1. *Consider N well-separated absorbing arcs for (1.1) of length εl_j for $j = 1, \ldots, N$ centered at $x_j \in \partial\Omega$. Then, the asymptotic solution to (1.1) is given in the outer region $|x - x_j| \gg \mathcal{O}(\varepsilon)$ for $j = 1, \ldots, N$ by*

$$(2.11a) \qquad v \sim -\pi \sum_{i=1}^N A_i G(x; x_i) + \chi.$$

Here G is the surface Green's function satisfying (2.5), and $\mathcal{A}^T = (A_1, \ldots, A_N)$ is the solution of the linear system

$$(2.11\text{b}) \qquad \left(I + \pi \mathcal{U} \left(I - \frac{1}{\bar{\mu}} E \mathcal{U} \right) \mathcal{G} \right) \mathcal{A} = \frac{|\Omega|}{D\pi N\bar{\mu}} \mathcal{U} e \,, \qquad E \equiv \frac{1}{N} e e^T \,.$$

In addition, the constant χ, representing the spatial average of v, is determined in terms of $\mathcal{A}$ and μ_j of (2.4b) by

$$(2.11\text{c}) \qquad \bar{v} \equiv \chi = \frac{|\Omega|}{D\pi N\bar{\mu}} + \frac{\pi}{N\bar{\mu}} e^T \mathcal{U} \mathcal{G} \mathcal{A} \,, \qquad \bar{\mu} \equiv \frac{1}{N} \sum_{j=1}^{N} \mu_j \,.$$

We first remark that our asymptotic solution to (1.1) in Principal Result 2.1 has in effect "summed" all of the logarithmic correction terms in the expansion of the solution, leaving an error that is transcendentally small in ε. Second, the constant χ in (2.11a), as given in (2.11c), has the immediate interpretation as the MFPT averaged with respect to an initial uniform distribution of starting points in Ω for the random walk.

For $\mu_j \ll 1$ we can solve (2.11b) and (2.11c) asymptotically by calculating the approximate inverse of the matrix multiplying $\mathcal{A}$ in (2.11b). This yields that

$$\mathcal{A} \sim \frac{|\Omega|}{ND\pi\bar{\mu}} \left[\mathcal{U} e - \pi \mathcal{U} \mathcal{G} \mathcal{U} e + \frac{\pi}{\bar{\mu}} \mathcal{U} E \mathcal{U} \mathcal{G} \mathcal{U} e \right] + \mathcal{O}(|\mu|^2) \,,$$

$$\chi \sim \frac{|\Omega|}{ND\pi\bar{\mu}} + \frac{|\Omega|}{N^2 D\bar{\mu}^2} e^T \mathcal{U} \mathcal{G} \mathcal{U} e + \mathcal{O}(|\mu|) \,.$$

Here $\mathcal{O}(|\mu|^p)$ indicates terms that are proportional to μ_j^p. In this way, we obtain the following two-term result.

PRINCIPAL RESULT 2.2. *For $\varepsilon \ll 1$, a two-term expansion for the solution of (1.1) is provided by (2.11a), where A_j and χ are given explicitly by*

$$(2.12\text{a}) \qquad A_j \sim \frac{|\Omega|\mu_j}{ND\pi\bar{\mu}} \left(1 - \pi \sum_{i=1}^{N} \mu_i \mathcal{G}_{ij} + \frac{\pi}{N\bar{\mu}} p_w(x_1, \ldots, x_N) \right) + \mathcal{O}(|\mu|^2) \,,$$

$$(2.12\text{b}) \qquad \bar{v} \equiv \chi \sim \frac{|\Omega|}{ND\pi\bar{\mu}} + \frac{|\Omega|}{N^2 D\bar{\mu}^2} p_w(x_1, \ldots, x_N) + \mathcal{O}(|\mu|) \,.$$

Here $p_w(x_1, \ldots, x_N)$ is the following weighted discrete sum defined in terms of the entries $\mathcal{G}_{ij}$ of the Green's function matrix of (2.10):

$$(2.13) \qquad p_w(x_1, \ldots, x_N) \equiv \sum_{i=1}^{N} \sum_{j=1}^{N} \mu_i \mu_j \mathcal{G}_{ij} \,, \qquad \mu_j = -\frac{1}{\log(\varepsilon d_j)} \,, \qquad d_j = \frac{l_j}{4} \,.$$

Hence, the average MFPT χ is minimized for an arrangement of arcs that minimize the discrete sum $p_w(x_1, \ldots, x_N)$.

Consider the case of exactly one absorbing arc with length $|\partial\Omega_{\varepsilon_1}| = 2\varepsilon$ for which $d = 1/2$. Then, (2.11a) and (2.12b) for $v(x)$ and the average MFPT χ, respectively, reduce to

$$(2.14)$$
$$v(x) \sim \frac{|\Omega|}{D\pi} \left[-\log\left(\frac{\varepsilon}{2}\right) + \pi \left(R(x_1; x_1) - G(x; x_1) \right) \right] \,,$$
$$\bar{v} = \chi \sim \frac{|\Omega|}{D\pi} \left[-\log\left(\frac{\varepsilon}{2}\right) + \pi R(x_1; x_1) \right] \,.$$

Here $G(x; x_1)$ is the Green's function satisfying (2.5) with regular part $R(x_1; x_1)$. These results are the generalizations to an arbitrary domain Ω with smooth boundary $\partial\Omega$ of the results given in [18] for the case of the unit disk.

Another relevant special case of Principal Result 2.2 is when there are N well-separated absorbing arcs of a common length εl with the arcs arranged on $\partial\Omega$ in such a way that $\mathcal{G}$ is a cyclic matrix. For instance, this situation occurs when there are exactly two arcs of the same length on the boundary of the unit disk or when N arcs of a common length are arranged with equidistant spacing on the boundary of the unit disk. When $\mathcal{G}$ is cyclic, then

$$(2.15) \qquad \mathcal{G}e = \frac{p}{N}e\,, \qquad p \equiv p(x_1, \ldots, x_N) \equiv \sum_{i=1}^{N}\sum_{j=1}^{N}\mathcal{G}_{ij}\,,$$

where $e^T = (1, \ldots, 1)$. For this special case, the exact solution to (2.11b) and (2.11c) is simply

$$(2.16) \qquad \begin{aligned} A_j &= \frac{|\Omega|}{ND\pi}\,, \quad j = 1, \ldots, N\,; \\ \bar{v} &\equiv \chi = \frac{|\Omega|}{ND\pi\mu} + \frac{|\Omega|}{N^2 D}p(x_1, \ldots, x_N)\,, \qquad \mu = \frac{-1}{\log[(\varepsilon l/4)]}\,. \end{aligned}$$

This result for χ effectively sums all of the logarithmic terms in powers of μ. In addition, (2.11a) for v becomes

$$(2.17) \qquad v(x) \sim \frac{|\Omega|}{ND\pi}\left[-\log\left(\frac{\varepsilon l}{4}\right) + \frac{\pi}{N}p(x_1, \ldots, x_N) - \pi\sum_{j=1}^{N}G(x; x_j)\right].$$

We remark that the analysis leading to Principal Results 2.1 and 2.2 has assumed that the absorbing windows on the boundary are well separated in the sense that $|x_i - x_j| = \mathcal{O}(1)$ for $i \neq j$. Next, we briefly consider the case where there are M_j nonoverlapping absorbing arcs clustered in an $\mathcal{O}(\varepsilon)$ ball near some point $x_j^* \in \partial\Omega$ for $j = 1, \ldots, N$, where N now denotes the number of clusters and $M_1 + \cdots + M_N = n$ is the total number of absorbing windows. To allow for the effect of the clustering of absorbing windows, we need only replace μ_j in Principal Results 2.1 and 2.2 with $-1/\log(\varepsilon d_j)$, where d_j is to be determined from the far-field behavior of the following inner problem:

$$(2.18a) \qquad v_{\eta\eta} + v_{ss} = 0\,, \quad \eta \geq 0\,, \quad -\infty < s < \infty\,,$$

$$(2.18b) \quad v = 0\,, \quad \eta = 0, \, s \in S_{jk}\,; \qquad \partial_\eta v = 0\,, \quad \eta = 0, \, s \notin S_{jk}\,, \quad k = 1, \ldots, M_j\,,$$

$$(2.18c) \qquad v \sim \log|y| - \log d_j + o(1) \quad \text{as} \quad |y| = \left(\eta^2 + s^2\right)^{1/2} \to \infty\,.$$

Here, for each $j = 1, \ldots, N$, S_{jk} are a collection of M_j nonoverlapping finite intervals of lengths l_{jk} for $k = 1\ldots, M_j$. Although the constant d_j is determined uniquely by the solution to (2.18), it must, in general, be computed numerically. However, d_j can be determined analytically for the special case of a cluster of exactly two absorbing windows of a common length l_j, with edge separation $2a_j$, so that $S_{j1} = \{s \mid -a_j - l_j < s < -a_j\}$ and $S_{j2} = \{s \mid a_j < s < a_j + l_j\}$. For this symmetric two-window cluster, (2.18) is readily solved analytically by first using symmetry to reduce the problem to the quarter plane $\eta, s > 0$ and then using the simple analytic mapping

$Z = z^2$, where $z = s + i\eta$. This leads to an explicitly solvable half-plane problem $\text{Im}(Z) > 0$ with one absorbing window. In this way, we obtain for the symmetric two-window cluster that d_j is given explicitly by

$$(2.19) \qquad d_j = \frac{l_j}{2}\left[1 + \frac{2a_j}{l_j}\right]^{1/2}.$$

For $a_j = 0$, then $d_j = l_j/2$, which corresponds to the value of d_j in (2.2) for an absorbing window of length $2l_j$.

We conclude that the results in Principal Results 2.1 and 2.2 still hold provided that whenever we have a two-window cluster of a common length we replace $\mu_j = -1/\log(\varepsilon l_j/4)$ in those results with $\mu_j = -1/\log(\varepsilon d_j)$, where d_j is given in (2.19). Therefore, Principal Results 2.1 and 2.2 are readily modified to explicitly treat any combination of well-separated windows and symmetric two-window clusters on the domain boundary.

Finally, we show that our result for the average MFPT $\bar{v}$ for a symmetric two-window cluster makes a smooth transition to the corresponding result for $\bar{v}$ for the case of two well-separated windows. For simplicity, we assume that there are exactly two absorbing windows each of length l on the boundary. Then, from (2.12b), we obtain that

$$(2.20a) \qquad \bar{v} \sim \frac{|\Omega|}{D\pi}\left[-\log(\varepsilon d_1) + \pi R_*\right] \qquad \text{(a two-window cluster)},$$

$$(2.20b) \qquad \bar{v} \sim \frac{|\Omega|}{D\pi}\left[-\frac{1}{2}\log\left(\frac{\varepsilon l}{4}\right) + \frac{\pi}{4}\left(R(x_1;x_1) + R(x_2;x_2) + 2G(x_1;x_2)\right)\right]$$
$$\text{(two well-separated windows)}.$$

Here $x_1^* \in \partial\Omega$ is the center of the two-window cluster, $R_* \equiv R(x_1^*, x_1^*)$ is the regular part of the Green's function at x_1^*, and d_1 is given in (2.19). In the overlap region $\mathcal{O}(\varepsilon) \ll |x_2 - x_1| \ll 1$, the well-separated result (2.20b) can be simplified using $R_{11} \approx R_{22} \approx R_*$ and $G(x_1;x_2) \sim -\pi^{-1}\log|x_1 - x_2| + R_*$. In this same overlap region, we simplify the cluster result (2.20a) by using $d_1 \sim \frac{l}{2}(2a/l)^{1/2}$ for $a/l \gg 1$, where $2a + l \approx |x_2 - x_1|/\varepsilon$. Since both limiting results lead to the common expression

$$(2.21)$$
$$\bar{v} \sim \frac{|\Omega|}{D\pi}\left[-\frac{1}{2}\log\left(\frac{\varepsilon l}{4}\right) - \frac{\pi}{2}\log|x_2 - x_1| + \pi R_*\right] \qquad \text{for } \mathcal{O}(\varepsilon) \ll |x_2 - x_1| \ll \mathcal{O}(1),$$

we conclude that there is a smooth transition between the two results in (2.20). As a remark, for the special case of the unit disk, where the regular part R has the uniform value $R = 1/(8\pi)$ (see (3.2)) everywhere on the domain boundary, the results (2.20) are readily seen to agree asymptotically with the result in equation (29) of [11] and provide the missing $\mathcal{O}(1)$ terms not given in this latter result of [11].

3. Numerical realizations. In subsections 3.1 and 3.2 we apply the results of section 2 to the unit disk and the unit square, respectively. For these domains, $G(x;\xi)$ and $R(\xi;\xi)$ can be calculated analytically from (2.5). For other more general domains, in subsection 3.3 we present and implement a boundary integral numerical method to numerically calculate $G(x;\xi)$ and $R(\xi;\xi)$. In this section we will assume throughout that the absorbing windows are well separated in the sense that $|x_i - x_j| = \mathcal{O}(1)$ for $i \neq j$.

3.1. The unit disk. Let Ω be the unit disk, $\Omega \equiv \{x \mid |x| \leq 1\}$. When $\xi \in \Omega$, so that the singularity is in the interior of the domain, the Neumann Green's function $G(x;\xi)$ with $\int_\Omega G(x;\xi)\,dx = 0$ is well known (see equation (4.3a) of [12]):

$$(3.1) \qquad G(x;\xi) = \frac{1}{2\pi}\left(-\log|x-\xi| - \log\left|x|\xi| - \frac{\xi}{|\xi|}\right| + \frac{1}{2}(|x|^2 + |\xi|^2) - \frac{3}{4}\right).$$

By letting ξ approach a point on $\partial\Omega$ in (3.1), we obtain that the surface Green's function solution of (2.5) is

$$(3.2) \qquad G(x;\xi) = -\frac{1}{\pi}\log|x-\xi| + \frac{|x|^2}{4\pi} - \frac{1}{8\pi}, \qquad R(\xi;\xi) = \frac{1}{8\pi}.$$

We now apply the results of section 2 to the unit disk. We first assume that there is one absorbing patch of length $|\partial\Omega_{\varepsilon_1}| = 2\varepsilon$ on $\partial\Omega$. Then, with G and R as given in (3.2) and using $|\Omega| = \pi$, (2.14) becomes

$$(3.3)$$
$$v(x) = \mathrm{E}\left[\tau \mid X(0) = x\right] \sim \frac{1}{D}\left[-\log\varepsilon + \log 2 + \frac{1}{4} + \log|x - x_1| - \frac{|x|^2}{4}\right],$$
$$\chi \sim \frac{1}{D}\left[-\log\varepsilon + \log 2 + \frac{1}{8}\right].$$

The formula for $\bar{v} = \chi$ in (3.3) agrees with that in equation (1.3) of [18]. If we fix the center of the absorbing arc at $x_1 = (1,0)$ and let $x = (\xi, 0)$ be the initial point for the random walk, then a simple calculation from (3.3) shows that v is maximized when $\xi = -1$, i.e., at the farthest point in Ω to the absorbing arc centered at $(1,0)$. In Figure 2(a) we use (3.3) to plot v versus ξ, where $x = (\xi, 0)$. Finally, to compare our results with those in [18], we let $x_1 = (1,0)$ and take $x = (0,0)$ and $x = (-1,0)$ as two choices for the initial point x for the random walk. Then, (3.3) yields

$$(3.4)$$
$$\mathrm{E}\left[\tau \mid X(0) = (0,0)\right] \sim \frac{1}{D}\left[-\log\varepsilon + \log 2 + \frac{1}{4}\right],$$
$$\mathrm{E}\left[\tau \mid X(0) = (-1,0)\right] \sim \frac{1}{D}\left[-\log\varepsilon + 2\log 2\right],$$

which agree with the results given in equations (1.2) and (1.4) of [18].

Next, we assume that there are exactly two well-separated absorbing arcs on the boundary of the unit disk, each with length $|\partial\Omega_{\varepsilon_j}| = 2\varepsilon$. We fix the location of one of the arcs at $x_1 = (1,0)$ and we let the other arc be centered at some $x_2 = (\cos\theta, \sin\theta)$, where $0 < \theta < \pi$ is a parameter. For this special case the matrix $\mathcal{G}$ is cyclic. Therefore, the average MFPT can be calculated from (2.16) and (3.2). In addition, for an initial starting point at the origin, i.e., $x(0) = 0$, then (2.17) with $G(0;x_j) = -1/(8\pi)$ determines $v(0)$. In this way, we get

$$(3.5) \qquad \chi \sim \frac{1}{2D}\left(-\log\varepsilon + \frac{1}{4} + \frac{1}{2}\log 2 - \frac{1}{2}\log(1 - \cos\theta)\right), \qquad v(0) \sim \chi + \frac{1}{8D}.$$

For $\varepsilon = 0.05$, in Figure 2(b) we plot $v(0)$ versus the polar angle θ for the location of the second absorbing arc. This plot shows that the specific MFPT $v(0)$ is minimized when the two absorbing arcs are antipodal, as expected intuitively. It also shows that $v(0)$ varies rather significantly as a function of the relative locations of the two absorbing arcs.
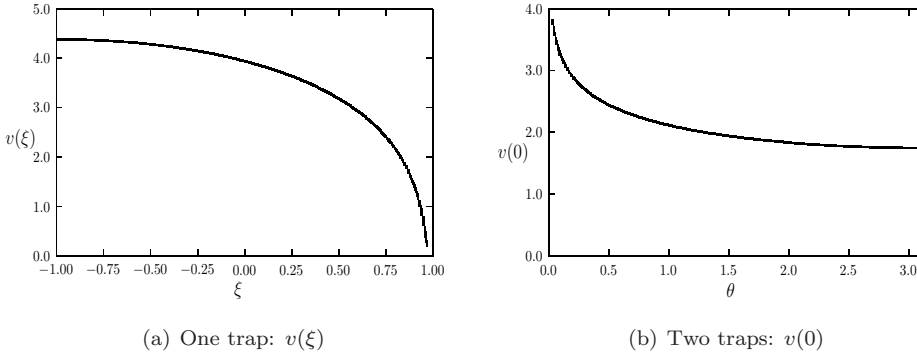
(a) One trap: $v(\xi)$ (b) Two traps: $v(0)$

FIG. 2. *Left figure: plot of v given in* (3.3) *versus the horizontal coordinate* $x = (\xi, 0)$ *for the case of one absorbing arc centered at* $x_1 = (1, 0)$. *Right figure: plot of* $v(0)$ *versus* θ *given in* (3.5) *for the case of two absorbing arcs centered at* $x_1 = (1, 0)$ *and* $x_2 = (\cos\theta, \sin\theta)$. *For both figures, $\varepsilon = 0.05$ and $D = 1$.*

Next, we consider the case of N absorbing arcs centered at $x_1, \ldots, x_N$ on the boundary of the unit disk having a common length $|\partial\Omega_{\varepsilon_j}| = 2\varepsilon$ for $j = 1, \ldots, N$. Then, from (3.2) and (2.12b), the average MFPT is

$$(3.6) \qquad \bar{v} = \chi \sim \frac{1}{DN}\left[-\log\left(\frac{\varepsilon}{2}\right) + \frac{N}{8} - \frac{1}{N}\sum_{i=1}^{N}\sum_{j \neq i}^{N}\log|x_i - x_j|\right].$$

The sum in (3.6) is minimized when $x_j = e^{2\pi ij/N}$, for $j = 1, \ldots, N$, are the Nth roots of unity. For this choice of x_j, the Green's function matrix $\mathcal{G}$ is cyclic and the results in (2.15), (2.16), and (2.17) apply. We obtain $G(x_i; x_j)$ and $R(x_j; x_j)$ from (3.2) and then calculate $p(x_1, \ldots, x_N)$ as

$$p(x_1, \ldots, x_N) = \sum_{i=1}^{N}\sum_{j=1}^{N}\mathcal{G}_{ij} = \frac{N^2}{8\pi} - \frac{1}{\pi}\sum_{k=1}^{N}\sum_{j \neq k}^{N}\log|x_j - x_k|$$

$$(3.7) \qquad = \frac{N^2}{8\pi} - \frac{1}{\pi}\sum_{k=1}^{N}\log\left[\prod_{\substack{j=1 \\ j \neq k}}^{N}\left(1 - e^{2\pi i(j-k)/N}\right)\right] = \frac{1}{\pi}\left(\frac{N^2}{8} - N\log N\right),$$

where we have used the simple identity $\prod_{\substack{j=1 \\ j \neq k}}^{N}\left(x - ye^{2\pi i(j-k)/N}\right) = \left|x^{N-1}\left(1 + \frac{y}{x} + \cdots + \left(\frac{y}{x}\right)^{N-1}\right)\right|$.

Therefore, for the special case $x_j = e^{2\pi ij/N}$ for $j = 1, \ldots, N$ we obtain from (3.7), (2.16), and (2.17) that

(3.8)

$$v(x) \sim \frac{1}{DN}\left[-\log\left(\frac{\varepsilon N}{2}\right) + \frac{N}{8} - \pi\sum_{j=1}^{N}G(x; x_j)\right], \quad \chi \sim \frac{1}{DN}\left[-\log\left(\frac{\varepsilon N}{2}\right) + \frac{N}{8}\right],$$

where $G(x; \xi)$ is given in (3.2). Note that χ in (3.8) agrees with (3.3) when $N = 1$ and (3.5) when $N = 2$ and $\theta = \pi$. As remarked following (2.16), the error associated with the asymptotic result (3.8) is smaller than any power of μ.

We now show that the result (3.8) for a periodic arrangement of boundary traps agrees with the corresponding result that can be obtained from the dilute fraction limit of homogenization theory, whereby the mixed Dirichlet–Neumann boundary condition on the boundary of the unit disk is replaced by an effective Robin boundary condition, as was studied in [14]. From equations (2.6) and (4.3) of [14], the homogenized problem for the MFPT is to find $v_h(x)$ satisfying

$$(3.9a) \qquad \triangle v_h = -\frac{1}{D}, \quad r = |x| \leq 1; \qquad \varepsilon \partial_r v_h + \kappa v_h = 0, \quad r = 1,$$

where κ is defined in terms of the length fraction σ of traps by (see equation (4.3) of [14])

$$(3.9b) \qquad \kappa \equiv -\frac{\pi\sigma}{2} \left(\log \left[\sin \left(\frac{\pi\sigma}{2} \right) \right] \right)^{-1}.$$

The homogenization result $v_h(0)$ for the MFPT for escape starting from the center of the unit disk is readily calculated from (3.9) as

$$(3.10) \qquad v_h(0) = \frac{1}{D} \left[\frac{1}{4} - \frac{\varepsilon}{\pi\sigma} \log \left(\sin \left[\frac{\pi\sigma}{2} \right] \right) \right].$$

In contrast, we obtain from (3.8), upon using $G(0; x_j) = -1/(8\pi)$ from (3.2), that

$$(3.11) \qquad v(0) \sim \frac{1}{D} \left[\frac{1}{4} - \frac{1}{N} \log \left(\frac{\varepsilon N}{2} \right) \right].$$

Since the trap length fraction on the boundary of the unit disk is $\sigma = 2\varepsilon N/(2\pi) = \varepsilon N/\pi$, we observe that the dilute fraction limit $\varepsilon N \ll 1$ of the homogenization result (3.10) agrees with (3.11).

Finally, we illustrate the significant effect on χ resulting from different placements of the absorbing arcs on the boundary of the unit disk. We consider either three or four absorbing arcs, each of length 2ε, so that $\mu = (-\log[\varepsilon/2])^{-1}$. For an arbitrary arrangement of the centers x_j, for $j = 1, \dots, N$ of the arcs, the two-term asymptotic expansion for the average MFPT χ is given in (3.6), which has an error of $\mathcal{O}(\mu)$. When the x_j are chosen to be at the roots of unity, the simple result (3.8) for χ holds, which has an error of $\mathcal{O}(\mu^k)$ for any $k > 0$. Finally, for an arbitrary arrangement of x_j, the asymptotic result for χ that has an error $\mathcal{O}(\mu^k)$ for any $k > 0$ is given in (2.11c) of Principal Result 2.1. Upon using (3.2) for $G(x_i; x_j)$ and R, we can readily show that (2.11b) and (2.11c) reduce to

$$(3.12) \qquad \chi \sim \frac{1}{DN} \left(-\log \left(\frac{\varepsilon}{2} \right) + \frac{N}{8} - \frac{1}{N} e^T \mathcal{G}_1 \left[I - \mu \left(I - E \right) \mathcal{G}_1 \right]^{-1} e \right).$$

Here $E = N^{-1} e e^T$, $e^T = (1, \dots, 1)$, I is the $N \times N$ identity matrix, and $\mathcal{G}_1$ is defined as the $N \times N$ symmetric matrix with $\mathcal{G}_{1jj} = 0$ for $j = 1, \dots, N$ and $\mathcal{G}_{1ij} = \log |x_i - x_j|$ for $i \neq j$. For $N = 3$, in Figure 3(a) we compare the two-term asymptotic result (3.6) with the more accurate result (3.12) as a function of ε for three different placements of absorbing arcs on the boundary of the unit disk (see the caption of Figure 3(a)). A similar comparison for $N = 4$ is made in Figure 3(b). These results show that the two-term approximation (3.6) is rather accurate for small ε and that the effect on χ of the locations of the absorbing arcs is rather significant even for rather small values of ε.

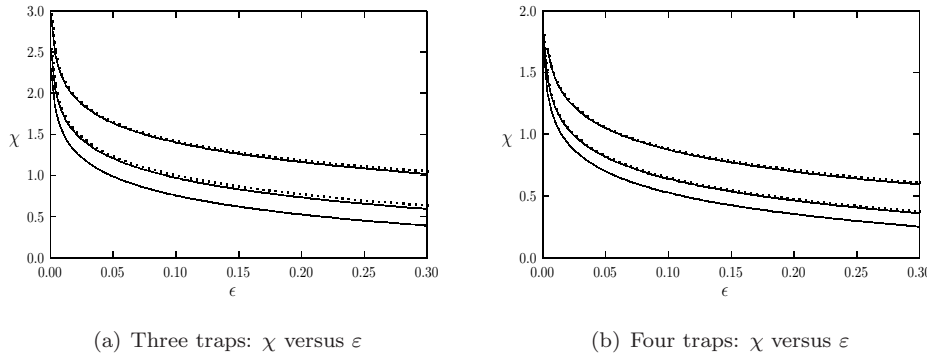(a) Three traps: χ versus ε (b) Four traps: χ versus ε

FIG. 3. *Comparison of the two-term result for χ given in (3.6) (dotted curves) with the log-summed result (3.12) (solid curves) versus ε for $D = 1$ and for traps on the boundary of the unit disk. Left figure: $N = 3$ traps at $x_1 = e^{\pi i/3}$, $x_2 = e^{\pi i/2}$, $x_3 = e^{2\pi i/3}$ (top curves); $x_1 = e^{\pi i/6}$, $x_2 = e^{\pi i/2}$, $x_3 = e^{5\pi i/6}$ (middle curves); $x_1 = e^{-\pi i/3}$, $x_2 = e^{\pi i/2}$, $x_3 = e^{4\pi i/3}$ (bottom curves). Right figure: $N = 4$ traps at $x_1 = e^{\pi i/6}$, $x_2 = e^{\pi i/3}$, $x_3 = e^{2\pi i/3}$, $x_4 = e^{5\pi i/6}$ (top curves); $x_1 = (1,0)$, $x_2 = e^{\pi i/3}$, $x_3 = e^{2\pi i/3}$, $x_4 = (-1,0)$ (middle curves); $x_1 = e^{\pi i/4}$, $x_2 = e^{3\pi i/4}$, $x_3 = e^{5\pi i/4}$, $x_4 = e^{7\pi i/4}$ (bottom curves). When the traps are centered at the roots of unity (bottom curves in both figures), the results (3.6) and (3.12) are identical.*

3.2. The unit square. For the unit square Ω, we must calculate the surface Green's function satisfying (2.5) with a singularity $\xi \in \partial\Omega$. To do so, we proceed by first calculating the Neumann Green's function $G(x; \xi)$ for $\xi \in \Omega$ and then taking the limit as ξ approaches a boundary point. The Green's function with an interior singularity satisfies

(3.13)
$$\triangle G = \frac{1}{|\Omega|} - \delta(x - \xi), \quad x \in \Omega; \qquad \partial_n G = 0, \quad x \in \partial\Omega; \qquad \int_\Omega G(x; \xi)\, dx = 0.$$

In this subsection we label $x = (x_1, x_2)$ as the observation point in $\Omega \equiv \{(x_1, x_2) \mid 0 < x_1 < 1, \, 0 < x_2 < 1\}$, while the singular point has coordinates $\xi = (\xi_1, \xi_2)$.

The function $G(x; \xi)$ can be readily represented in terms of an eigenfunction expansion. Then, certain infinite series can be summed analytically to extract the slowly converging part of the series resulting from the logarithmic singularity. In this way, in equation (4.13) of [13] it was found that

(3.14a)
$$G(x; \xi) = -\frac{1}{2\pi} \log|x - \xi| + R(x; \xi),$$

where the regular part $R(x; \xi)$ is given explicitly by

(3.14b) $R(x; \xi) = -\dfrac{1}{2\pi} \displaystyle\sum_{n=0}^{\infty} \log\left(|1 - q^n z_{+,+}||1 - q^n z_{+,-}||1 - q^n z_{-,+}||1 - q^n \zeta_{+,+}|\right)$

$$-\frac{1}{2\pi} \sum_{n=0}^{\infty} \log(|1 - q^n \zeta_{+,-}||1 - q^n \zeta_{-,+}||1 - q^n \zeta_{-,-}|)$$

$$-\frac{1}{2\pi} \log \frac{|1 - z_{-,-}|}{|r_{-,-}|} + H(x_1, \xi_1) - \frac{1}{2\pi} \sum_{n=1}^{\infty} \log|1 - q^n z_{-,-}|.$$

Here the eight complex constants $z_{\pm,\pm}$ and $\zeta_{\pm,\pm}$ are defined in terms of additional

complex constants $r_{\pm,\pm}$, $\rho_{\pm,\pm}$ by

(3.15a) $\quad z_{\pm,\pm} \equiv e^{\pi r_{\pm,\pm}}, \quad \zeta_{\pm,\pm} \equiv e^{\pi \rho_{\pm,\pm}}, \quad q \equiv e^{-2\pi} < 1,$

(3.15b) $\quad r_{+,\pm} \equiv -|x_1 + \xi_1| + i(x_2 \pm \xi_2), \quad r_{-,\pm} \equiv -|x_1 - \xi_1| + i(x_2 \pm \xi_2),$

(3.15c) $\quad \rho_{+,\pm} \equiv |x_1 + \xi_1| - 2 + i(x_2 \pm \xi_2), \quad \rho_{-,\pm} \equiv |x_1 - \xi_1| - 2 + i(x_2 \pm \xi_2).$

In (3.14) and (3.15), $|\omega|$ is the modulus of the complex number ω. In (3.14b), $H(x_1, \xi_1)$ is defined by

(3.16) $\qquad H(x_1, \xi_1) \equiv \frac{1}{12}\left[h(x_1 - \xi_1) + h(x_1 + \xi_1)\right], \qquad h(\theta) \equiv 2 - 6|\theta| + 3\theta^2.$

Now suppose that the singular point is located on the bottom side of the square so that $\xi = (\xi_1, 0)$ with $0 < \xi_1 < 1$. Then, the term $\log|1 - z_{-,+}|$ in (3.14b) also has a singularity at $x = (\xi_1, 0)$ and must be extracted from the sum. In this case, the explicit solution to (2.5) is obtained by rewriting (3.14) as

(3.17a) $\qquad G(x; \xi) = -\frac{1}{\pi}\log|x - \xi| + R(x; \xi),$

where the regular part $R(x; \xi)$ is given explicitly by

(3.17b) $\quad R(x; \xi) = -\frac{1}{2\pi}\sum_{n=0}^{\infty}\log\left(|1 - q^n z_{+,+}||1 - q^n z_{+,-}||1 - q^n \zeta_{+,+}|\right)$

$$-\frac{1}{2\pi}\sum_{n=0}^{\infty}\log(|1 - q^n \zeta_{+,-}||1 - q^n \zeta_{-,+}||1 - q^n \zeta_{-,-}|)$$

$$-\frac{1}{2\pi}\log\frac{|1 - z_{-,-}|}{|r_{-,-}|} - \frac{1}{2\pi}\log\frac{|1 - z_{-,+}|}{|r_{-,+}|} + H(x_1, \xi_1)$$

$$-\frac{1}{2\pi}\sum_{n=1}^{\infty}\log\left(|1 - q^n z_{-,-}||1 - q^n z_{-,+}|\right).$$

The self-interaction term $R(\xi; \xi)$ is obtained by taking the limit $x \to \xi$ in (3.17b). By using L'Hôpital's rule to calculate the terms $\log|1 - z_{-,\pm}|/|r_{-,\pm}|$, we obtain with $q = e^{-2\pi}$ that

(3.18) $\qquad R(\xi; \xi) = -\frac{1}{\pi}\sum_{n=0}^{\infty}\log\left[\left(1 - q^n e^{-2\xi_1 \pi}\right)\left(1 - q^n e^{-2\pi(1-\xi_1)}\right)\right]$

$$-\frac{2}{\pi}\sum_{n=0}^{\infty}\log(1 - q^n) - \frac{\log \pi}{\pi} + \left(\xi_1 - \frac{1}{2}\right)^2 + \frac{1}{12}.$$

Similarly, $G(x; \xi)$ and $R(\xi; \xi)$ can be found when the singular point is on any of the other three sides of the square.

We now calculate the MFPT for a few special cases. We first suppose that there is one absorbing window of length 2ε centered at the midpoint $\xi = (0.5, 0)$ of the bottom side of the square. We consider initial points for a random walk that are located on the vertical line $x = (0.5, x_2)$, where $0 < x_2 < 1$. For this configuration, (2.14) yields

(3.19) $\qquad v(x) \sim \frac{1}{D\pi}\left[-\log\left(\frac{\varepsilon}{2}\right) + \pi\left(R(\xi; \xi) - G(x; \xi)\right)\right],$

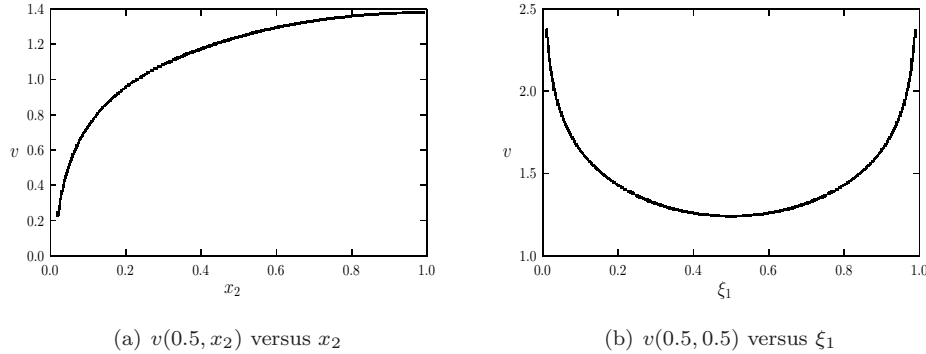(a) $v(0.5, x_2)$ versus x_2 (b) $v(0.5, 0.5)$ versus ξ_1

FIG. 4. *Left figure: plot of the MFPT $v(0.5, x_2)$ on $0 < x_2 < 1$ given in (3.19) when there is one trap located at $\xi = (0.5, 0.0)$ at the midpoint of the bottom side of the unit square. Right figure: plot of the MFPT $v(0.5, 0.5)$, with initial point at the center of the unit square, versus the x-coordinate of a trap location that slides along the bottom of the square at position $\xi = (\xi_1, 0)$ with $0 < \xi_1 < 1$. For both figures, $D = 1$, $\varepsilon = 0.02$, and the trap has length 2ε.*

where $G(x; \xi)$ and $R(\xi; \xi)$ is given in (3.17) and (3.18), respectively. In Figure 4(a) we plot v versus x_2, where we show that v increases as the initial point tends to the top boundary of the square, i.e., $x_2 \to 1$. Next, suppose that the initial point is at the center of the unit square, i.e., $x = (0.5, 0.5)$, but that the center $\xi = (\xi_1, 0)$ of the absorbing window slides along the bottom of the unit square with $0 < \xi_1 < 1$. Upon using (3.19), in Figure 4(b) we plot v versus ξ_1 on $0 < \xi_1 < 1$, which shows that v is minimized at $\xi_1 = 0.5$, as expected intuitively.

Next, we suppose that the initial point is at the center $x = (0.5, 0.5)$ of the unit square but that there are two traps, each of length 2ε, on the boundary of the square. We fix the center of one of the traps at the midpoint $\xi_1 = (0.0, 0.5)$ of the left boundary, and we let the center ξ_2 of the other trap slide along the boundary of the square in a counterclockwise direction starting from ξ_1. From (2.12) and (2.11a), the MFPT is given asymptotically by

$$(3.20) \qquad v(x) \sim \frac{1}{2D\pi} \left[-\log\left(\frac{\varepsilon}{2}\right) + \frac{\pi}{2} \left(R(\xi_1; \xi_1) + R(\xi_2, \xi_2) + 2G(\xi_1; \xi_2) \right) \right. \\ \left. - \pi \left(G(x; \xi_1) + G(x; \xi_2) \right) \right].$$

In Figure 5 we plot $v(x)$ versus the distance s along the boundary of the location of the second trap relative to the first trap. Although the analysis in section 2 leading to (3.20) is not valid for trap locations that are $\mathcal{O}(\varepsilon)$ close to the corner points of the square, we observe in Figure 5 that v has peaks as ξ_2 approaches these corner points, corresponding to $s = 0.5$, $s = 1.5$, and $s = 2.5$. In addition, as seen from Figure 5, v has a global minimum when $\xi_2 = (1.0, 0.5)$ (i.e., $s = 2.0$), corresponding to a configuration of two traps that are equally spaced on the boundary of the square.

Finally, we consider the special case with one absorbing window centered at the corner of the unit square. Since the window is centered at a nonsmooth part of the boundary, we must modify the analysis for the MFPT in section 2. Choosing $\xi = (0, 0)$ as the corner point, we first calculate $G(x; \xi)$ from (3.14) as

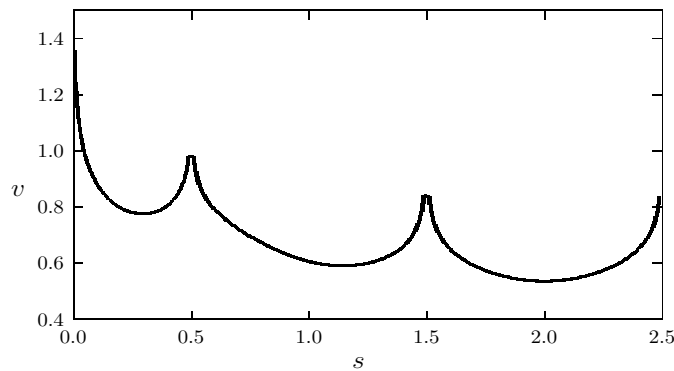$$(3.21a) \qquad G(x; \xi) = -\frac{2}{\pi} \log |x| + R(x; 0),$$

FIG. 5. *Plot of the MFPT $v(0.5, 0.5)$, with initial point at the center of the unit square, when there are two traps on the boundary of the unit square. The first trap is fixed at $\xi_1 = (0.0, 0.5)$ on the left side of the square, while the second trap starts from ξ_1 and then slides around the boundary of the square in a counterclockwise direction. The plot shows $v(0.5, 0.5)$ as a function of the distance s along the boundary of the second trap relative to ξ_1 for $0 < s < 2.5$. When $s = 2$, then the second trap is at $(1.0, 0.5)$. At this antipodal point, $v(0.5, 0.5)$ has a global minimum. The local maxima at $s = 0.5$, $s = 1.5$, and $s = 2.5$ occur when the second trap is close to a corner of the square. We took $\varepsilon = 0.02$ and $D = 1$, and each trap has length 2ε.*

where the regular part $R(x; 0)$ is given explicitly by

$$(3.21b) \quad R(x; 0) = -\frac{1}{2\pi} \sum_{n=1}^{\infty} \log \left(|1 - q^n z_{+,+}| |1 - q^n z_{+,-}| |1 - q^n z_{-,+}| |1 - q^n z_{-,-}| \right)$$

$$- \frac{1}{2\pi} \sum_{n=0}^{\infty} \log \left(|1 - q^n \zeta_{+,+}| |1 - q^n \zeta_{+,-}| |1 - q^n \zeta_{-,+}| |1 - q^n \zeta_{-,-}| \right)$$

$$- \frac{1}{2\pi} \log \left(\frac{|1 - z_{+,+}|}{|r_{+,+}|} \frac{|1 - z_{+,-}|}{|r_{+,-}|} \frac{|1 - z_{-,+}|}{|r_{-,+}|} \frac{|1 - z_{-,-}|}{|r_{-,-}|} \right) + H(x_1, 0).$$

Moreover, the self-interaction term $R(0; 0)$ is given by

$$(3.22) \qquad R(0; 0) = -\frac{4}{\pi} \sum_{n=1}^{\infty} \log \left(1 - q^n \right) - \frac{2 \log \pi}{\pi} + \frac{1}{3}, \qquad q = e^{-2\pi}.$$

The analysis in section 2 is easily modified to treat an absorbing arc centered at a corner of the square. We obtain that

$$(3.23)$$
$$\triangle v = -\frac{1}{D}, \quad x \in \Omega; \qquad \partial_n v = 0, \quad x \in \partial\Omega \backslash \{0\}; \quad v \sim \frac{A_1}{\mu} + A_1 \log |x| \quad \text{as } x \to 0.$$

Since $\partial\Omega$ has a $\pi/2$ corner at $x = 0$, the divergence theorem yields $A_1 = 2|\Omega|/(D\pi)$, and hence

$$(3.24) \qquad\qquad\qquad v = -\frac{|\Omega|}{D} G(x; 0) + \chi.$$

The constant χ is obtained by expanding v as $x \to 0$. We use $G(x; 0) \sim -2\pi^{-1} \log |x| + R(0; 0)$ and then compare the resulting expression with the singularity behavior in

(3.23). In this way, in place of (2.14), we get

(3.25)
$$v \sim \frac{2|\Omega|}{D\pi}\left[-\log(\varepsilon d) + \frac{\pi}{2}\left(R(0;0) - G(x;0)\right)\right], \qquad \bar{v} \sim \frac{2|\Omega|}{D\pi}\left[-\log(\varepsilon d) + \frac{\pi}{2}R(0;0)\right].$$

Here $|\Omega| = \pi$, while $R(0;0)$ and $G(x;0)$ are given in (3.22) and (3.21), respectively. Finally, the constant d in (3.25), inherited from the far-field behavior of the inner problem, depends on the details of how the absorbing arc of length 2ε is placed near the corner. If the arc is on only one side so that $v = 0$ on $0 < x_1 < 2\varepsilon$ with $x_2 = 0$, then $d = 1$. If $v = 0$ on the two sides $x_2 = 0$, $0 < x_1 < \varepsilon$, and $x_1 = 0$, $0 < x_2 < \varepsilon$, then $d = 1/4$.

By solving certain integral equations asymptotically, a result for $\bar{v}$ was obtained in [19] for the unit square when an absorbing arc of length ε is placed on $x_2 = 0$, $0 < x_1 < \varepsilon$, near the corner at the origin. For this configuration, $d = 1/2$ in (3.25). Upon approximating $R(0;0)$ in (3.22) by taking only the first term in the infinite sum, (3.25) reduces approximately to $\bar{v} \sim 2D^{-1}\left[\log 2 - \log(\pi\varepsilon) + 2e^{-2\pi} + \pi/6\right]$, in agreement with equation (2.8) of [19].

3.3. More general domains: A boundary integral method. For an arbitrary bounded domain with smooth boundary $\partial\Omega$, we now describe a boundary integral scheme to compute the surface Neumann Green's function $G(x;x_0)$ satisfying

(3.26a)
$$\triangle G(x;x_0) = \frac{1}{|\Omega|}, \quad x \in \Omega, \quad x_0 \in \partial\Omega,$$

(3.26b)
$$\partial_n G(x;x_0) = \delta(x - x_0), \quad x \in \partial\Omega; \qquad \int_\Omega G(x;x_0)\,dx = 0.$$

In terms of $G(x;x_0)$ we then define the regular part, or self-interaction term, $R(x_0;x_0)$ by

(3.26c)
$$\lim_{x \to x_0}\left(G(x;x_0) + \frac{1}{\pi}\log|x - x_0|\right) = R(x_0;x_0).$$

Requiring only the discretization of the domain boundary, the boundary element method (BEM) is well suited to numerically solve problems with singular boundary terms. However, the need to impose the uniqueness condition $\int_\Omega G(x;x_0)\,dx = 0$ negates the benefit of the BEM derived from restricting the discretization to the boundary. Since (3.26) for G without this integral constraint defines G only up to an arbitrary constant, one approach would be to compute any specific solution for G and then determine the constant to add to G by an a posteriori area integration.

We choose to adopt an alternative numerical approach, which is based on a regularization of (3.26). To this end, we consider the following reduced wave equation in which β is taken to be a small parameter and $x_0 \in \partial\Omega$:

(3.27)
$$L_\beta G_\beta(x;x_0) \equiv \triangle G_\beta(x;x_0) - \beta^2 G_\beta(x;x_0) = 0, \quad x \in \Omega;$$
$$\partial_n G_\beta(x;x_0) = \delta(x - x_0), \quad x \in \partial\Omega.$$

To determine the relationship between (3.26) and (3.27), we expand the solution to (3.27) for $\beta \ll 1$ as

(3.28)
$$G_\beta(x;x_0) = \frac{1}{\beta^2}G_0(x;x_0) + G_1(x;x_0) + \beta^2 G_2(x;x_0) + \cdots.$$

Substituting (3.28) into (3.27) and collecting powers of β^2, we get that G_0 is a constant and that G_1 and G_2 satisfy

(3.29a) $\quad \triangle G_1(x; x_0) = G_0(x; x_0), \quad x \in \Omega; \qquad \partial_n G_1(x; x_0) = \delta(x - x_0), \quad x \in \partial\Omega,$

(3.29b) $\quad \triangle G_2(x; x_0) = G_1(x; x_0), \quad x \in \Omega; \qquad \partial_n G_2(x; x_0) = 0, \quad x \in \partial\Omega.$

Upon applying the divergence theorem to (3.29a) we obtain that $G_0(x; x_0) = |\Omega|^{-1}$. A similar application of the divergence theorem to (3.29b) shows that G_1 must satisfy the solvability condition $\int_\Omega G_1(x; x_0) \, dx = 0$. Therefore, $G_1(x; x_0)$ is precisely the surface Neumann Green's function satisfying (3.26). Since $G_0(x; x_0) = |\Omega|^{-1}$ is known, our strategy is to use Richardson extrapolation in which we solve (3.27) numerically for two distinct values of $\beta \ll 1$ and then eliminate the $\mathcal{O}(\beta^2)$ term to yield an approximation of $G_1(x; x_0)$ which is accurate up to $\mathcal{O}(\beta^4)$ terms.

   The starting point for the boundary integral equation for (3.27) is the Green's identity associated with the operator L_β in (3.27), given by $\int_\Omega (u_1 L_\beta u_2 - u_2 L_\beta u_1) \, dx = \int_{\partial\Omega} (u_1 \partial_n u_2 - u_2 \partial_n u_1) \, ds$. We choose $u_1 = G_\beta(x; x_0)$ and $u_2 = g_\beta(x; \xi) \equiv \frac{1}{2\pi} K_0(\beta |x - \xi|)$ as the free space Green's function satisfying $L_\beta g_\beta(x; \xi) = -\delta(x - \xi)$ with $\xi \in \Omega$, where $K_0(z)$ is the modified Bessel function of the second kind of order zero. Then, Green's identity reduces to

(3.30) $\qquad G_\beta(\xi; x_0) + \int_{\partial\Omega} G_\beta(x; x_0) \, \partial_n g_\beta(x; \xi) \, ds(x) = \frac{1}{2\pi} K_0(\beta |x_0 - \xi|).$

Next, we decompose $G_\beta(x; x_0)$ into the sum of a singular part and a regular part $R_\beta(x; x_0)$ as

(3.31) $\qquad\qquad G_\beta(x; x_0) = -\frac{1}{\pi} \log |x - x_0| + R_\beta(x; x_0).$

Upon substituting (3.31) into (3.30), we obtain the following integral relation for ξ in the interior of Ω, i.e., $\xi \in \Omega$:

(3.32)
$$R_\beta(\xi; x_0) + \int_{\partial\Omega} R_\beta(x; x_0) \partial_n g_\beta(x; \xi) \, ds(x) = \frac{1}{2\pi} K_0(\beta |x_0 - \xi|)$$
$$+ \frac{1}{\pi} \log |x_0 - \xi| + \frac{1}{\pi} \int_{\partial\Omega} \log |x - x_0| \, \partial_n g_\beta(x; \xi) \, ds(x).$$

To derive an integral equation from (3.32) that involves only unknown quantities on the boundary, we consider the local behavior of the integrals in (3.32) in the limit as $\xi \to \partial\Omega$. Let ξ be located on the smooth boundary $\partial\Omega$ and consider the integral $\int_{\partial\Omega_\varepsilon(\xi)} f(x) \partial_n g_\beta(x; \xi) \, ds(x)$. Here $\partial\Omega_\varepsilon(\xi)$ represents the boundary $\partial\Omega$ of the domain in which the boundary points in the vicinity of ξ have been deformed to form a semicircular arc of radius ε which is centered at ξ and which is such that ξ is incorporated within the boundary of $\partial\Omega_\varepsilon(\xi)$. Under the assumption that f is continuous at ξ, the contribution to the integral on the semicircular arc can be calculated for $\varepsilon \to 0$ as

$$\lim_{\varepsilon \to 0} \int_{-\pi/2}^{\pi/2} f(\xi_1 + \varepsilon \cos\theta, \xi_2 + \varepsilon \sin\theta) \frac{\beta}{2\pi} K_0'(\beta\varepsilon) \varepsilon \, d\theta = -\frac{1}{2} f(\xi_1, \xi_2).$$

Therefore, for boundary points where $\xi \in \partial\Omega$, we have

(3.33) $\qquad \lim_{\varepsilon \to 0} \int_{\partial\Omega_\varepsilon(\xi)} f(x) \partial_n g_\beta(x; \xi) \, ds(x) = -\frac{1}{2} f(\xi) + \fint_{\partial\Omega} f(x) \partial_n g_\beta(x; \xi) \, ds(x).$

Here $\fint_{\partial\Omega}$ represents the exclusion of a small symmetric region from the boundary in the neighborhood of the point ξ upon taking the limit to zero, as is customary in the definition of Cauchy principal value integrals. Making use of the limiting behavior (3.33) in (3.32), we obtain the following boundary integral equation for $R_\beta(\xi; x_0)$:

$$
\begin{aligned}
\text{(3.34)} \quad \frac{1}{2}R_\beta(\xi; x_0) + &\fint_{\partial\Omega} R_\beta(x; x_0)\partial_n g_\beta(x; \xi)\, ds(x) = \frac{1}{2\pi}K_0(\beta\,|x_0 - \xi|) \\
&+ \frac{1}{2\pi}\log|x_0 - \xi| + \frac{1}{\pi}\fint_{\partial\Omega}\log|x - x_0|\,\partial_n g_\beta(x; \xi)\, ds(x)\,.
\end{aligned}
$$

For the special case $\xi \to x_0$ the first two singular terms on the right-hand side of (3.34) have the asymptotic behavior

$$
\begin{aligned}
\lim_{\xi \to x_0} \left(\frac{1}{2\pi}K_0(\beta\,|x_0 - \xi|) + \frac{1}{2\pi}\log|x_0 - \xi| \right) \\
= \frac{1}{2\pi}\left[-\gamma + \log\left(\frac{2}{\beta}\right) \right] + \mathcal{O}\left(|x_0 - \xi|^2 \log|x_0 - \xi| \right),
\end{aligned}
$$

where γ is Euler's constant.

Next, we discretize the boundary integral equation (3.34). We approximate the boundary by N circular arcs, and on each arc we assume a piecewise quadratic representation of the unknown function

$$
R_\beta(x(t); x_0) = \sum_{j=1}^{3} R_j(x_0)N_j(t)\,, \qquad N_j(t) = \prod_{\substack{k=1 \\ k \neq j}}^{3} \frac{(t - t_k)}{(t_j - t_k)}\,.
$$

Here t is the standard parameterization of the arc, and $N_j(t)$ are the quadratic Lagrange basis functions associated with the collocation points t_j, which are chosen to be the zeros of the third degree Legendre polynomial. The boundary integral equation (3.34) then assumes the discrete form

$$
\begin{aligned}
\frac{1}{2}R_k^m(x_0) + \sum_{n=1}^{N}\sum_{j=1}^{3} R_j^n(x_0)\fint_{\partial\Omega_n} N_j(t)\partial_n g_\beta(x(t), \xi_k)\, ds(t) = \frac{1}{2\pi}K_0(\beta\,|x_0 - \xi_k|) \\
+ \frac{1}{2\pi}\log|x_0 - \xi_k| + \frac{1}{\pi}\sum_{n=1}^{N}\fint_{\partial\Omega_n}\log|x(t) - x_0|\,\partial_n g_\beta(x(t), \xi_k)\, ds(t)\,.
\end{aligned}
$$

This dense linear system can be written compactly in index form as

$$
\text{(3.35)} \quad \frac{1}{2}R_k^m(x_0) + \sum_{n=1}^{N}\sum_{j=1}^{3}\mathcal{K}_{kj}^{mn}R_j^n(x_0) = b_k^m + \mathcal{L}_k^m\,,
$$

where

$$
\mathcal{K}_{kj}^{mn} = \begin{cases}
\dfrac{-a\beta}{2\pi}\fint_{-\alpha_n}^{\alpha_n} N_j^n(t)K_1\left(2a\beta\sin\left(\frac{|t - t_k^m|}{2}\right)\right)\sin\left(\frac{|t - t_k^m|}{2}\right) dt\,, & m = n\,, \\[2.5ex]
\dfrac{-a\beta}{2\pi}\int_{-\alpha_n}^{\alpha_n} N_j^n(t)\dfrac{K_1(\beta r_k^{mn}(t))}{r_k^{mn}(t)}\left(a - \bar{\xi}_{1,k}^{mn}\cos t - \bar{\xi}_{2,k}^{mn}\sin t\right) dt\,, & m \neq n\,,
\end{cases}
$$

$$
b_k^m = \frac{1}{2\pi}\begin{cases}
-\gamma + \log\frac{2}{\beta}\,, & \xi_k = x_0\,, \\[1.5ex]
K_0(\beta\,|x_0 - \xi_k|) + \log|x_0 - \xi_k|\,, & \xi_k \neq x_0\,,
\end{cases}
$$

and $K_1(z)$ is the modified Bessel function of the second kind of order one. In addition,

$$
\mathcal{L}_k^m = -\frac{a\beta}{2\pi^2} \sum_{n=1}^{N} \begin{cases}
\fint_{-\alpha_n}^{\alpha_n} \log\left(2a\sin\left(\frac{|t|}{2}\right)\right) K_1\left(2a\beta\sin\left(\frac{|t-t_k^m|}{2}\right)\right) \sin\left(\frac{|t-t_k^m|}{2}\right) dt\,, \\
\qquad m = n\,,\ n = n_0\,, \\
\int_{-\alpha_n}^{\alpha_n} \log\left(2a\sin\left(\frac{|t|}{2}\right)\right) \frac{K_1(\beta r_k^{mn}(t))}{r_k^{mn}(t)} \left(a - \bar\xi_{1,k}^{mn}\cos t - \bar\xi_{2,k}^{mn}\sin t\right) dt\,, \\
\qquad m \neq n\,,\ n = n_0\,, \\
\fint_{-\alpha_n}^{\alpha_n} \log\left(r_0^n(t)\right) K_1\left(2a\beta\sin\left(\frac{|t-t_k^m|}{2}\right)\right) \sin\left(\frac{|t-t_k^m|}{2}\right) dt\,, \\
\qquad m = n\,,\ n \neq n_0\,, \\
\int_{-\alpha_n}^{\alpha_n} \log\left(r_0^n(t)\right) \frac{K_1(\beta r_k^{mn}(t))}{r_k^{mn}(t)} \left(a - \bar\xi_{1,k}^{mn}\cos t - \bar\xi_{2,k}^{mn}\sin t\right) dt\,, \\
\qquad m \neq n\,,\ n \neq n_0\,.
\end{cases}
$$

Here a represents the local radius of curvature of the nth element, $\bar\xi_{j,k}^{mn}$ represents the jth component of the kth collocation point in the mth receiving element relative to the local coordinate system centered on the nth element, $r_k^{mn}(t)$ represents the distance between the current integration point t in the nth element and the kth collocation point in the mth receiving element, $r_0^n(t)$ is the distance between the current integration point t in the nth sending element and the source point x_0, and n_0 represents the element number in which the source point x_0 is located at the middle collocation point. The integrals in (3.35) are performed using adaptive Gauss–Konrod integration.

The numerical solution to the linear system (3.35) yields approximate numerical values for $R_\beta(x; x_0)$ for $x \in \partial\Omega$ and for $R_\beta(x_0; x_0)$. The function $R_\beta(x; x_0)$ for an interior point with $x \in \Omega$ is obtained from (3.32), which then determines $G_\beta(x; x_0)$ from (3.31). A Richardson extrapolation applied to (3.28) then determines the surface Neumann Green's function $G(x; x_0)$. Our final step in our BEM scheme is to use Richardson extrapolation to extract the regular part $R(x_0; x_0)$ of the surface Neumann Green's function, defined in (3.26c) from the small β expansion

$$
(3.36) \qquad R_\beta(x_0; x_0) = \frac{1}{|\Omega|\beta^2} + R(x_0; x_0) + \mathcal{O}(\beta^2)\,.
$$

Some numerical results computed from the BEM are given below and in section 4.

The unit disk. In order to establish the convergence rate of the BEM we first consider the unit disk for which $R(x_0; x_0) = 1/(8\pi) = 0.039789$, as obtained from the analytical result (3.2). In Table 1 we give numerical BEM results showing that the convergence rate of our numerical scheme is $\mathcal{O}\left(N^{-3}\right)$.

TABLE 1

Numerical BEM results approximating the regular part $R(x_0; x_0) = 1/8\pi$ of the surface Neumann Green's function for the unit disk with N boundary elements. The convergence rate of the numerical scheme is $\mathcal{O}\left(N^{-3}\right)$.

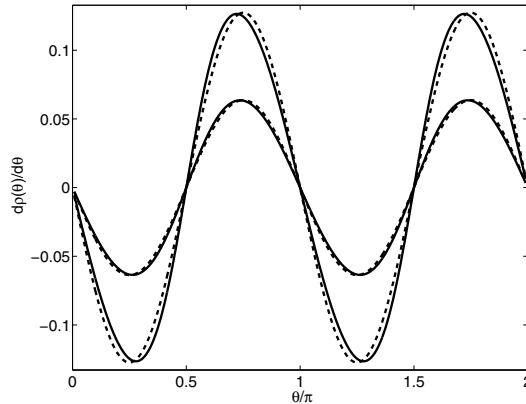|	$R_\beta(x_0; x_0)$		$R(x_0; x_0)$	
N	$\beta = 0.025$	$\beta = 0.0125$	Extrapolated value	Exact value
32	0.037515	0.039091	0.040666	0.039789
64	0.037243	0.038576	0.039908	0.039789
128	0.037203	0.038501	0.039799	0.039789
256	0.037198	0.038491	0.039783	0.039789

FIG. 6. *Comparison of $\rho'(\theta) \equiv \frac{d}{d\theta} R(x_0(\theta), x_0(\theta))$ versus θ/π from the analytical perturbation result (3.37) (dashed curves) and the numerical BEM results (solid curves) for a near unit disk with boundary $r = 1 + \delta \cos(2\theta)$ with $\delta = 0.1$ (large amplitude curves) and $\delta = 0.05$ (small amplitude curves). In the BEM scheme, $N = 128$ elements were used.*

A perturbation of the unit disk. We consider a perturbation of the unit disk with the boundary defined by $r = 1 + \delta \cos(2\theta)$, where $\delta > 0$ is small. For a source point at position $x_0(\theta) = (r \cos \theta, r \sin \theta)$ on the boundary, we define the self-interaction term $\rho(\theta)$ by $\rho(\theta) \equiv R(x_0(\theta), x_0(\theta))$. From Principal Result 4.3, which is proved in the appendix, we obtain for $\delta \ll 1$ that

$$(3.37) \qquad\qquad \rho'(\theta) \sim -\frac{4\delta}{\pi} \sin(2\theta) + \mathcal{O}(\delta^2) \,.$$

In Figure 6 we show a very favorable comparison between the asymptotic result (3.37) for $\delta = 0.05$ and $\delta = 0.1$ and the corresponding full numerical BEM results for $\rho'(\theta)$ computed with $N = 128$ elements. In computing $\rho'(\theta)$ from the BEM scheme, we used a not-a-knot cubic spline to perform the numerical differentiation. Figure 6 gives further supporting evidence that the BEM scheme is able to compute $\rho(\theta)$ accurately.

An ellipse. Next, we let Ω be the ellipse with boundary $x(\theta) = 2 \cos \theta$ and $y(\theta) = \sin \theta$. By allowing the source point $x_0(\theta) = (\cos \theta, \sin \theta)$ to move around the boundary, in Figure 7(a) we plot the BEM result for $\rho(\theta) \equiv R(x_0(\theta), x_0(\theta))$ versus θ/π with $N = 128$ elements. The curvature $\kappa(\theta)$ of the boundary is also shown in this figure. For this example, the local maxima of $\rho(\theta)$ and $\kappa(\theta)$ coincide. Next, we compute the MFPT for the case of one absorbing window of length 2ε on the boundary of the ellipse centered at $x_0(\theta)$. Upon setting $|\Omega| = 2\pi$ in (2.14), and with a minor change in notation from (2.14), the average MFPT $\bar{v}(\theta)$ and the MFPT $v(\theta; x)$ for a starting position $x \in \Omega$ are given by

(3.38)
$$\bar{v}(\theta) \sim 2 \left[-\log \left(\frac{\varepsilon}{2} \right) + \pi \rho(\theta) \right] ; \qquad v(\theta; x) \sim 2 \left[-\log \left(\frac{\varepsilon}{2} \right) + \pi \left(\rho(\theta) - G(x; x_0(\theta)) \right) \right] .$$

We define $v_1(\theta) \equiv v(\theta; x)$ for an initial point at the origin $x = (0, 0)$ and $v_2(\theta) = v(\theta; x)$ for the initial point $x = (1, 0)$. In Figure 7(b) we plot $\bar{v}$, v_1, and v_2 versus θ/π when $\varepsilon = 0.05$. From this figure it is seen that the MFPT depends significantly on both the location θ of the absorbing window on the boundary of the ellipse and on the chosen initial point inside the ellipse for the random walk.
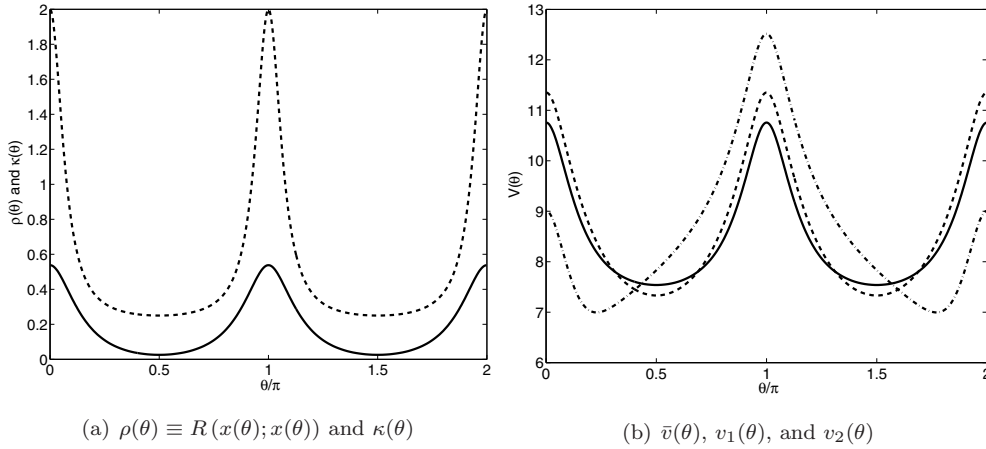
(a) $\rho(\theta) \equiv R\left(x(\theta); x(\theta)\right)$ and $\kappa(\theta)$

(b) $\bar{v}(\theta)$, $v_1(\theta)$, and $v_2(\theta)$

FIG. 7. *Left figure: plot of $\rho(\theta) \equiv R(x_0(\theta), x_0(\theta))$ (solid curve) versus θ/π and the boundary curvature $\kappa(\theta)$ (dashed curve) for an elliptical region with boundary $x = 2\cos\theta$, $y = \sin\theta$. Right figure: plot of the average MFPT $\bar{v}(\theta)$ versus θ/π (solid curve) together with the MFPTs $v_1(\theta)$ (dashed curve) and $v_2(\theta)$ (dash-dotted curve), as defined in (3.38), for a random walk with initial starting point $x = (0,0)$ and $x = (1,0)$, respectively. The absorbing window of length 2ε with $\varepsilon = 0.05$ is centered at polar angle θ on $\partial\Omega$.*

4. Optimization of the principal eigenvalue.
In this section we asymptotically calculate the principal eigenvalue for

$$(4.1a) \qquad \triangle u + \lambda u = 0, \quad x \in \Omega, \qquad \int_\Omega u^2\, dx = 1,$$

$$(4.1b) \qquad \partial_n u = 0, \quad x \in \partial\Omega_r; \qquad u = 0, \quad x \in \partial\Omega_a \equiv \bigcup_{j=1}^N \partial\Omega_{\varepsilon_j}.$$

Here $\partial\Omega = \partial\Omega_r \cup \partial\Omega_a$ is a smooth boundary. We assume that there are N small well-separated absorbing arcs $\partial\Omega_{\varepsilon_j}$, each with length $|\partial\Omega_{\varepsilon_j}| = \varepsilon l_j \ll 1$, for which $\partial\Omega_{\varepsilon_j} \to x_j$ for $j = 1, \ldots, N$. We let $\lambda(\varepsilon)$ denote the first eigenvalue of (4.1), with corresponding eigenfunction $u(x, \varepsilon)$. Clearly, $\lambda(\varepsilon) \to 0$ as $\varepsilon \to 0$ with $u \to u_0 = |\Omega|^{-1/2}$.

To calculate $\lambda(\varepsilon)$ for $\varepsilon \ll 1$ we proceed as in section 2. In the inner region near the jth absorbing arc, we again obtain (2.2) as the inner problem. The far-field behavior of the solution to (2.2) is written as

$$(4.2) \qquad w_0 \sim \mu_j B_j \left[\log|y| - \log d_j + o(1)\right] \quad \text{as} \quad |y| \to \infty, \qquad d_j = l_j/4,$$

where $y = \varepsilon^{-1}(x - x_j)$, $\mu_j = -1/\log[\varepsilon d_j]$, and B_j is some unknown constant. This leads to a singularity behavior for the outer solution given by $u \sim B_j + \mu_j B_j \log|x - x_j|$ as $x \to x_j$ for $j = 1, \ldots, N$. In this way, we obtain that $\lambda(\varepsilon) = \lambda^* + \mathcal{O}(\varepsilon)$, where λ^* and u^* satisfy

$$(4.3a) \qquad \triangle u^* + \lambda^* u^* = 0, \qquad x \in \Omega; \qquad \partial_n u^* = 0, \qquad x \in \partial\Omega\backslash\{x_1, \ldots, x_N\},$$
$$(4.3b) \qquad u^* \sim B_j + \mu_j B_j \log|x - x_j| \quad \text{as} \quad x \to x_j, \quad j = 1, \ldots, N,$$

where μ_j is defined in (2.4b). The solution to (4.3) is written as

$$(4.4) \qquad u^* = -\pi \sum_{i=1}^{N} \mu_i B_i G_h(x; x_i)\,,$$

where $G_h(x; x_j)$ is the surface Helmholtz Green's function, which depends on λ^*, and satisfies

$$(4.5a) \qquad \triangle G_h + \lambda^* G_h = 0\,, \qquad x \in \Omega\,; \qquad \partial_n G_h = 0\,, \qquad x \in \partial\Omega \backslash \{x_j\}\,,$$

$$(4.5b) \qquad G_h(x; x_j) \sim -\frac{1}{\pi}\log|x - x_j| + R_h(x_j; x_j) \quad \text{as } x \to x_j \in \partial\Omega\,.$$

We then expand (4.4) as $x \to x_j$ and compare the resulting expression with the required singularity behavior (4.3b). This yields the following homogeneous linear system for the B_j for $j = 1, \ldots, N$:

$$(4.6) \qquad B_j + \pi\mu_j B_j R_{hj} + \pi \sum_{\substack{i=1 \\ i \neq j}}^{N} \mu_i B_i G_{hji} = 0\,, \qquad j = 1, \ldots, N\,.$$

Here we have defined $G_{hji} \equiv G_h(x_j; x_i)$, while $R_{hj} \equiv R_h(x_j; x_j)$ is the regular part of G_h given in (4.5). Upon writing this system in matrix form, we obtain the following main result.

PRINCIPAL RESULT 4.1. *Consider* (4.1) *for* N *well-separated absorbing arcs of length* $|\partial\Omega_{\varepsilon_j}| = \varepsilon l_j$ *centered at* $x_j \in \partial\Omega$ *for* $j = 1, \ldots, N$. *Then, the principal eigenvalue* $\lambda(\varepsilon)$ *of* (4.1) *satisfies* $\lambda(\varepsilon) = \lambda^* + \mathcal{O}(\varepsilon)$, *where* λ^* *is the smallest root of the transcendental equation*

$$(4.7) \qquad \text{Det}\,(I + \pi\mathcal{G}_h\mathcal{U}) = 0\,.$$

Here $\mathcal{U}$ *is the diagonal matrix as given in* (2.10), *and* $\mathcal{G}_h$ *is the Helmholtz Green's function matrix with entries*

$$(4.8) \qquad \mathcal{G}_{hjj} = R_h(x_j; x_j)\,, \quad j = 1, \ldots, N\,; \qquad \mathcal{G}_{hij} = G_h(x_i; x_j)\,, \quad i \neq j\,,$$

which are defined in terms of the solution $G_h(x; \xi)$ *and* $R_h(\xi; \xi)$ *to* (4.5). *The corresponding outer approximation to the principal eigenfunction is given in* (4.4), *where* $\mathcal{B}^T \equiv (B_1, \ldots, B_N)$ *is the eigenvector of* $(I + \pi\mathcal{G}_h\mathcal{U})\mathcal{B} = 0$.

The transcendental equation (4.7) has in effect summed all of the logarithmic terms in powers of μ_j for $\lambda(\varepsilon)$. To explicitly determine the first two terms in the logarithmic series, we let $\lambda^* \ll 1$ and obtain from (2.5) and (4.5) that
(4.9)
$$G_h(x; x_j) \sim -\frac{1}{\lambda^*|\Omega|} + G(x; x_j) + \mathcal{O}(\lambda^*)\,, \qquad R_h(x; x_j) \sim -\frac{1}{\lambda^*|\Omega|} + R(x; x_j) + \mathcal{O}(\lambda^*)\,.$$

Upon substituting (4.9) into (4.6), we obtain the approximating matrix eigenvalue problem
(4.10)
$$\mathcal{C}\mathcal{B} \sim \frac{\lambda^*|\Omega|}{\pi N}\mathcal{B}\,, \qquad \mathcal{C} \equiv (I + \pi\mathcal{G}\mathcal{U})^{-1}E\mathcal{U}\,, \qquad E \equiv \frac{1}{N}ee^T\,, \qquad e^T = (1, \ldots, 1)\,,$$

where $\mathcal{G}$ is the matrix in (2.10) involving the Green's function of (2.5). Since $\mathcal{C}$ is a rank one matrix, then for $\mu_j \ll 1$

$$\frac{\lambda^* |\Omega|}{\pi N} \sim \mathrm{Trace}\left[(I + \pi\mathcal{G}\mathcal{U})^{-1} E\mathcal{U}\right] \sim \mathrm{Trace}\left(E\mathcal{U}\right) - \pi\,\mathrm{Trace}\left[\mathcal{G}\mathcal{U}E\mathcal{U}\right]$$

$$= \bar{\mu} - \frac{\pi}{N}\sum_{i=1}^{N}\sum_{j=1}^{N}\mu_i\mu_j\mathcal{G}_{ij}\,.$$

The principal eigenfunction is found by substituting (4.9) for G_h into (4.4). We summarize the result as follows.

PRINCIPAL RESULT 4.2. *Let $\lambda(\varepsilon)$ be the principal eigenvalue of (4.1) with N well-separated absorbing arcs. Then, a two-term expansion for $\lambda(\varepsilon)$ is given by*

$$(4.11) \qquad \lambda(\varepsilon) \sim \lambda^* \sim \frac{\pi\bar{\mu}N}{|\Omega|} - \frac{\pi^2}{|\Omega|}p_w(x_1,\ldots,x_N) + \mathcal{O}(|\mu|^3)\,,$$

where $\bar{\mu} \equiv N^{-1}(\mu_1 + \cdots + \mu_N)$, $\mu_j = -1/\log[\varepsilon d_j]$ with $d_j = l_j/4$, and $p_w(x_1,\ldots,x_N)$ is the weighted discrete sum defined in (2.13). The corresponding two-term outer approximation to the principal eigenfunction is given by

$$(4.12) \qquad u \sim \frac{\pi}{\lambda^*|\Omega|}\sum_{i=1}^{N}\mu_i B_i - \pi\sum_{i=1}^{N}\mu_i B_i G(x; x_i) + \mathcal{O}(|\mu|^2)\,,$$

where $G(x; x_i)$ is the surface Green's function satisfying (2.5). For the special case $N = 1$, then

$$(4.13)\ \ \lambda(\varepsilon) \sim \lambda^* \sim \frac{\pi\mu_1}{|\Omega|} - \frac{\pi^2\mu_1^2}{|\Omega|}R(x_1; x_1) + \mathcal{O}(\mu_1^3)\,, \qquad \mu_1 \equiv -\frac{1}{\log[\varepsilon d_1]}\,, \quad d_1 = \frac{l_1}{4}\,.$$

As a special case of the result (4.11) for $\lambda(\varepsilon)$, suppose that Ω is the unit disk with N identical small absorbing arcs placed symmetrically around the boundary of the unit disk at the Nth roots of unity, i.e., $x_j = e^{2\pi ij/N}$. Then, with $|\Omega| = \pi$ and $p_w(x_1,\ldots,x_N) = \mu^2 p(x_1,\ldots,x_N)$, where $p(x_1,\ldots,x_N)$ is given in (3.7), (4.11) becomes

$$(4.14) \qquad \lambda(\varepsilon) \sim \mu N - \mu^2\left(\frac{N^2}{8} - N\log N\right) + \mathcal{O}(\mu^3)\,, \qquad \mu \equiv -\left(\log\left[\frac{\varepsilon l}{4}\right]\right)^{-1}\,.$$

As a further special case of (4.13), suppose that an absorbing arc of length 2ε is centered at $x_1 = (\xi_1, 0)$ on the bottom side of the unit square for which $R(x_1; x_1)$ is given explicitly from subsection 3.2 by the right-hand side of (3.18). Then, (4.13) with $d = 1/2$ and $|\Omega| = 1$ becomes

$$(4.15) \qquad \lambda(\varepsilon) \sim \pi\mu - \pi^2\mu^2 R(x_1; x_1)\,, \qquad \mu \equiv -\frac{1}{\log(\varepsilon/2)}\,.$$

In Figure 8(a) we plot $R(x_1; x_1)$ showing that it has a minimum when ξ_1 is at the midpoint of a side of the square. In Figure 8(b) we plot (4.15) versus ε for $\xi_1 = 0.5$, $\xi_1 = 0.3$, and $\xi_1 = 0.9$. The eigenvalue is largest when $\xi_1 = 0.5$.

(a) $R_1 \equiv R(x_1; x_1)$ with $x_1 = (\xi_1, 0)$ (b) $\lambda(\varepsilon)$
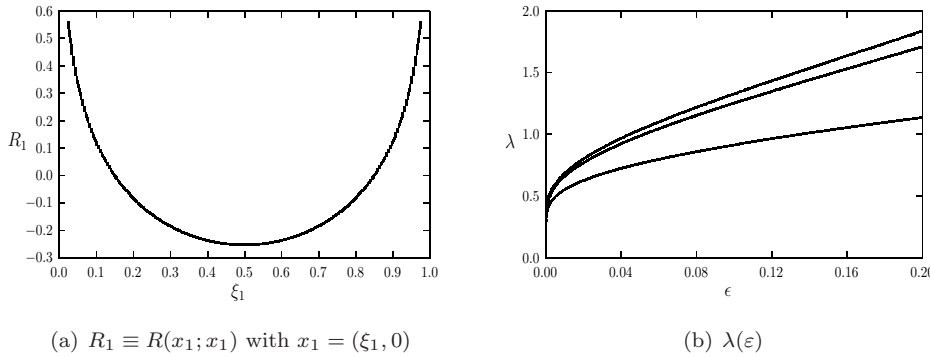
FIG. 8. *Left figure: plot of the regular part $R(x_1; x_1)$ of the Neumann Green's function for a square, as given in (3.18), with the trap centered on the bottom side of the square at $x_1 = (\xi_1, 0)$. Right figure: two-term expansion for $\lambda(\varepsilon)$ in (4.15) for $\xi_1 = 0.5$ (top curve), $\xi_1 = 0.3$ (middle curve), and $\xi_1 = 0.9$ (bottom curve). The eigenvalue is largest when $\xi_1 = 1/2$.*

The result (4.15) is not valid near a corner of the square, i.e., when $\xi_1 = \mathcal{O}(\varepsilon)$. For this case, where the arc is located at a corner of angle $\pi/2$, a modification of the analysis given in subsection 2.3 shows that

(4.16)
$$\lambda \sim \frac{\pi\mu}{2} - \frac{\pi^2\mu^2}{4} R(0;0), \quad \mu \equiv -\frac{1}{\log(\varepsilon d)}, \quad R(0;0) \equiv -\frac{4}{\pi} \sum_{n=1}^{\infty} \log\left(1-q^n\right) - \frac{2}{\pi}\log\pi + \frac{1}{3},$$

where $q = e^{-2\pi}$. The constant d, inherited from the inner problem, depends on the details of how the absorbing arc of length 2ε is placed near the corner. If the arc is on only one side so that $u = 0$ on $0 < x_1 < 2\varepsilon$ with $x_2 = 0$, then $d = 1$. If $u = 0$ on the two sides $x_2 = 0$, $0 < x_1 < \varepsilon$, and $x_1 = 0$, $0 < x_2 < \varepsilon$, then $d = 1/4$. In any case, it is clear by comparing (4.15) with (4.16) that λ is minimized when the absorbing arc is located at a corner of the square.

Next, we show that a few terms in the expansion for λ^* given in (4.11) of Principal Result 4.2 can be transformed directly into a few terms in the expansion for χ given in (2.12b) of Principal Result 2.2, in the sense that

(4.17)
$$\bar{v} = \chi = \frac{1}{D\lambda^*(\varepsilon)} + \mathcal{O}\left(|\mu|^2\right).$$

To establish (4.17) we first expand the solution to (1.1) in terms of all of the eigenfunctions $u_j(x, \varepsilon)$ and $\lambda_j(\varepsilon)$ for $j \geq 1$ of (4.1). In this notation the principal eigenpair $\lambda_1(\varepsilon)$ and $u_1(x, \varepsilon)$ is given asymptotically in (4.11) and (4.12), respectively. In the usual way, the eigenfunction expansion representation for v, and consequently $\bar{v} = \chi$, is

(4.18)
$$v = \frac{1}{D}\left[\frac{(u_1, 1)\,u_1}{\lambda_1\,(u_1, u_1)} + \sum_{j=2}^{\infty} \frac{(u_j, 1)\,u_j}{\lambda_j\,(u_j, u_j)}\right],$$

$$\chi = \bar{v} = \frac{1}{|\Omega|D}\left[\frac{(u_1, 1)^2}{\lambda_1\,(u_1, u_1)} + \sum_{j=2}^{\infty} \frac{(u_j, 1)^2}{\lambda_j\,(u_j, u_j)}\right].$$

Here $(u, v) \equiv \int_\Omega uv\,dx$. For $j \geq 2$, we use the divergence theorem to calculate $(\phi_j, 1)$ over the absorbing windows $\partial\Omega_a$ as $\lambda_j(\phi_j, 1) = -\int_{\partial\Omega_a} \partial_n\phi_j\,ds$, where $\lambda_j = \mathcal{O}(1)$ as

$\varepsilon \to 0$. Then, introducing the local coordinates $\hat{\eta} = \varepsilon^{-1}\eta$, $\hat{s} = \varepsilon^{-1}(s - s_j)$ and noting that $u_j = \mathcal{O}(|\mu|)$ in the inner region, as shown in (4.2), we estimate for $j \geq 2$ that

$$(u_j, 1) = -\frac{1}{\lambda_j} \sum_{j=1}^{N} \int_{\partial\Omega_j} \left(\varepsilon^{-1}\partial_{\hat{\eta}} u_j\right) \varepsilon d\hat{s} \sim \frac{1}{\lambda_j} \sum_{j=1}^{N} \int_{\partial\Omega_j} \mathcal{O}(|\mu|) \, d\hat{s} = \mathcal{O}(|\mu|).$$

Therefore, (4.18) reduces to

$$(4.19) \qquad v = \frac{1}{D\lambda_1}\frac{(u_1, 1)\,u_1}{(u_1, u_1)} + \mathcal{O}(|\mu|), \qquad \chi = \bar{v} \sim \frac{1}{|\Omega|D\lambda_1}\frac{(u_1, 1)^2}{(u_1, u_1)} + \mathcal{O}(|\mu|^2).$$

Next, we use (4.12) to calculate

$$(4.20) \qquad (u_1, 1) \sim \frac{\pi}{\lambda^*} \sum_{i=1}^{N} \mu_i B_i, \qquad (u_1, u_1) \sim \frac{\pi^2}{(\lambda^*)^2 |\Omega|} \sum_{i=1}^{N}\sum_{j=1}^{N} \mu_i \mu_j B_i B_j.$$

Upon substituting (4.20) and (4.12) into (4.19) and then using (4.11) for λ^*, we obtain that

$$v \sim \frac{1}{\lambda^* D} - \frac{|\Omega|}{D}\frac{\sum_{j=1}^{N} \mu_j B_j G(x; x_j)}{\sum_{j=1}^{N} \mu_j B_j} + \mathcal{O}(|\mu|), \qquad \chi = \bar{v} \sim \frac{1}{D\lambda^*} + \mathcal{O}(|\mu|^2),$$

$$(4.21) \quad v \sim \frac{|\Omega|}{\pi\bar{\mu}ND} + \frac{|\Omega|}{D\bar{\mu}^2 N^2}p_w(x_1, \ldots, x_N) - \frac{|\Omega|}{D}\frac{\sum_{j=1}^{N} \mu_j B_j G(x; x_j)}{\sum_{j=1}^{N} \mu_j B_j} + \mathcal{O}(|\mu|),$$

where $\bar{\mu} \equiv N^{-1}(\mu_1 + \cdots + \mu_N)$ and $p_w(x_1, \ldots, x_N)$ is defined in (2.13). This establishes the claim in (4.17). Finally, with regards to v, we use (4.10) to calculate $\mathcal{B}^T = (B_1, \ldots, B_N)$. To leading order for $\mu_j \ll 1$, (4.10) reduces to $\mathcal{EUB} \approx \bar{\mu}\mathcal{B}$, which yields $\mathcal{B}^T \sim (1, \ldots, 1)$. Therefore, upon setting $B_j \sim 1$ for $j = 1, \ldots, N$ in (4.21), we readily obtain that (4.21) agrees asymptotically with the result for the MFPT given in Principal Result 2.2.

4.1. An eigenvalue optimization problem. For the case of exactly one small (connected) absorbing arc of a fixed length εl, we now seek to determine the location of the center $x_0 \in \partial\Omega$ of this arc that minimizes the principal eigenvalue of (4.1). As stated in section 1, it was conjectured in section 1 of [3] that, for a general convex domain with a smooth boundary, an optimal absorbing arc must lie in a region of $\partial\Omega$ with large curvature. We first note that (4.13) shows that, up to $\mathcal{O}(\mu^2)$ terms, $\lambda(\varepsilon)$ is minimized at the global maximum of $R(x_0, x_0)$ for $x_0 \in \partial\Omega$. From (2.5) we introduce $R(x; x_0)$ by

$$(4.22) \qquad G(x; x_0) = -\frac{1}{\pi}\log|x - x_0| + R(x; x_0), \qquad x_0 \in \partial\Omega.$$

When Ω is a smooth perturbation of the unit disk, we will examine below whether maxima of $R(x_0; x_0)$ coincide with maxima of the curvature of the boundary. To do so, we require the following perturbation result determining the critical points of $R(x_0; x_0)$ for domains that are close to the unit disk.

PRINCIPAL RESULT 4.3. *Let Ω be a perturbation of the unit disk with boundary given in terms of polar coordinates by*

$$(4.23) \quad r = r(\theta) = 1 + \delta\sigma(\theta), \qquad \sigma(\theta) = \sum_{n=1}^{\infty}(a_n \cos(n\theta) + b_n \sin(n\theta)), \qquad \delta \ll 1.$$

Let $x_0 = x_0(\theta_0) = (r_0 \cos\theta_0, r_0 \sin\theta_0)$ be a point on the boundary, where $r_0 = 1 + \delta\sigma(\theta_0)$. For $x \in \partial\Omega$ we define

$$(4.24) \qquad \rho(\theta) = R(x; x_0) \qquad and \qquad \rho(\theta_0) \equiv R(x_0; x_0),$$

where $R(x; x_0)$ is the regular part of the Green's function in (4.22). Then, for $\delta \ll 1$, $\rho'(\theta_0)$ satisfies

$$(4.25) \qquad \rho'(\theta_0) = \frac{\delta}{\pi} \sum_{n=1}^{\infty} (n^2 + n - 2)(b_n \cos n\theta_0 - a_n \sin n\theta_0) + \mathcal{O}(\delta^2).$$

The proof of this result is given in the appendix. We now use Principal Result 4.3 to obtain the following result.

PRINCIPAL RESULT 4.4. *The maxima of $R(x_0, x_0)$ do not necessarily coincide with the maxima of the curvature $\kappa(\theta)$ of the boundary of a smooth perturbation of the unit disk. Consequently, for $\varepsilon \to 0$, $\lambda(\varepsilon)$ from (4.13) does not necessarily have a local minimum at the location of a local maximum of the curvature of a smooth boundary.*

To establish this result we take $a_2 = 1$, $a_3 = \mu$, with $a_n = 0$ for $n \neq 2, 3$ and $b_n = 0$ for $n \geq 1$ in (4.23), so that

$$(4.26) \qquad \sigma(\theta) = \cos(2\theta) + \mu\cos(3\theta).$$

For $\delta \ll 1$, the curvature κ of the boundary $r = 1 + \delta\sigma(\theta)$ is given by

$$(4.27) \qquad \kappa(\theta) = \frac{r^2 + 2r_\theta^2 - rr_{\theta\theta}}{(r^2 + r_\theta^2)^{3/2}} \sim 1 - \delta(\sigma + \sigma_{\theta\theta}) + \mathcal{O}(\delta^2).$$

Upon substituting (4.26) into (4.25) for $\rho'(\theta)$ and (4.27) for $\kappa(\theta)$, we obtain that

$$(4.28) \quad \kappa'(\theta) = -6\delta[\sin(2\theta) + 4\mu\sin(3\theta)], \qquad \rho'(\theta) = -\frac{4\delta}{\pi}\left[\sin(2\theta) + \frac{5\mu}{2}\sin(3\theta)\right].$$

We calculate that $\kappa'(\pi) = \rho'(\pi) = 0$ and

$$(4.29) \qquad \kappa''(\pi) = -6\delta[2 - 12\mu], \qquad \rho''(\pi) = -\frac{4\delta}{\pi}\left[2 - \frac{15\mu}{2}\right].$$

Thus, at $\theta = \pi$, κ has a maximum when $\mu < 1/6$ while ρ has a maximum when $\mu < 4/15$. Hence, for $\mu \in (\frac{1}{6}, \frac{4}{15})$, there is a point on $\partial\Omega$ where ρ has a local maximum at which κ has a local minimum. As a consequence, the principal eigenvalue of (4.1), given asymptotically in (4.13), does not in general have a local minimum when a small absorbing window is centered at a local maximum of the boundary curvature. This establishes Principal Result 4.4.

In Figure 9(a) we plot the domain when $\mu = 0.2$ and $\delta = 0.1$. For $\mu = 0.2$ and $\delta = 0.1$, in Figure 9(b) we plot $\kappa(\theta) - 1$, $r(\theta) - 1$, and the integral of the asymptotic result (4.28) for $\rho(\theta) - C$, where C is a constant of integration. For $\mu = 0.2$ and $\delta = 0.1$, in Figure 10 we show a very favorable comparison between the asymptotic result (4.28) for $\rho'(\theta)$ and the full numerical result for $\rho'(\theta)$ computed from the BEM scheme of subsection 3.3. The asymptotic and numerical results for $\rho'(\theta)$ are essentially indistinguishable in this plot. These numerical BEM results confirm the asymptotic prediction that, for $\mu = 0.2$ and $\delta \ll 1$, ρ has a local maximum while κ has a local minimum at $\theta = \pi$.

(a) perturbation of the unit disk

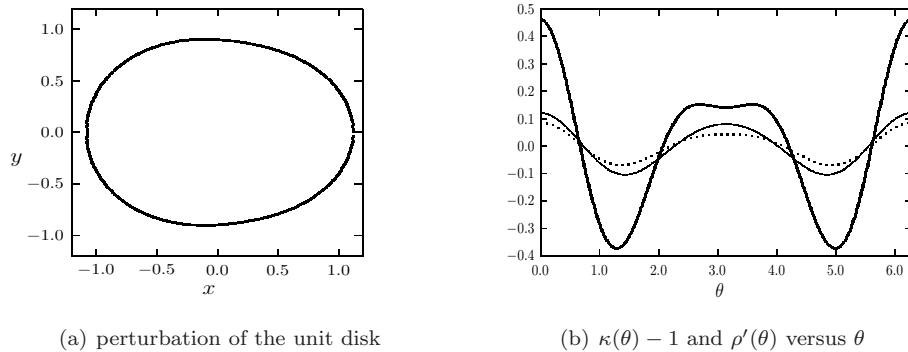(b) $\kappa(\theta) - 1$ and $\rho'(\theta)$ versus θ

FIG. 9. *Left figure: plot of the perturbed unit disk with boundary $r = 1 + \delta\left(\cos(2\theta) + \mu\cos(3\theta)\right)$ with $\delta = 0.1$ and $\mu = 0.2$. Right figure: plot of $\kappa(\theta) - 1$ (heavy solid line), $\delta\sigma(\theta)$ (solid line), and $\rho(\theta) - C$ (dotted line), where κ, σ, and ρ' are given in (4.27), (4.26), and (4.28), respectively. At $\theta = \pi$, the curvature has a local minimum and ρ has a local maximum.*
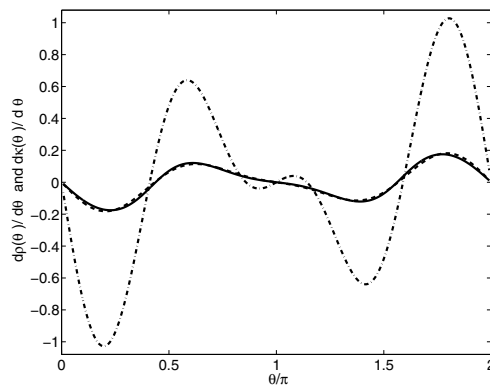

FIG. 10. *Plot of the derivative $\kappa'(\theta)$ (dash-dotted curve) of the near unit disk $r = 1 + \delta\left(\cos(2\theta) + \mu\cos(3\theta)\right)$ with $\delta = 0.1$ and $\mu = 0.2$ together with the asymptotic result (4.28) for $\rho'(\theta)$ (dashed curve) and the full numerical BEM result for $\rho'(\theta)$ (solid curve) with $N = 128$ elements. The asymptotic and numerical results for $\rho'(\theta)$ are very close.*

5. Conclusion. The method of matched asymptotic expansions was used to calculate the MFPT in an arbitrary two-dimensional domain with N asymptotically small absorbing windows on the domain boundary. Analytical results are given for the disk and the square for various arrangements of the small absorbing windows on the domain boundary. Similar results for the MFPT for more general domains were obtained by using a BEM to compute the surface Neumann Green's function.

An open problem is to calculate the dwell time (cf. [21]) in a two-dimensional domain with both asymptotically small absorbing windows on its boundary and traps of asymptotically small radii located inside the domain. An example of such a problem in the unit disk for the case of one concentric trap is considered in [21].

In Part II of this paper [5] we asymptotically calculate the MFPT for narrow escape from a spherical domain.

Appendix. The regular part of the surface Neumann Green's function for a perturbed disk. In this appendix we prove Principal Result 4.3. From (2.5)

and (4.22), we obtain that $R(x; x_0)$ satisfies
(A.1)
$$\triangle R(x; x_0) = \frac{1}{|\Omega|}, \qquad x \in \Omega; \qquad \nabla R(x; x_0) \cdot \hat{n} = \frac{1}{\pi} \frac{(x - x_0) \cdot \hat{n}}{|x - x_0|^2}, \qquad x \in \partial\Omega.$$

In polar coordinates we write $x_0 = (r_0 \cos\theta_0, r_0 \sin\theta_0)$, $x = (r\cos\theta, r\sin\theta)$, and $r_0 = r_0(\theta_0)$. We then calculate that $|x - x_0|^2 = r^2 + r_0^2 - 2rr_0 \cos(\theta - \theta_0)$, and

$$\hat{n} = \frac{1}{\sqrt{(r')^2 + r^2}} \begin{pmatrix} r' \sin\theta + r\cos\theta \\ -r'\cos\theta + r\sin\theta \end{pmatrix},$$

$$(x - x_0) \cdot \hat{n} = \frac{1}{\sqrt{(r')^2 + r^2}} \left[r^2 - r_0 r' \sin(\theta - \theta_0) - r_0 r \cos(\theta - \theta_0) \right].$$

By writing $r = 1 + \delta\sigma$ and $r_0 = 1 + \delta\sigma_0$, the right-hand side of the boundary condition in (A.1) becomes

(A.2) $$\frac{1}{\pi} \frac{(x - x_0) \cdot \hat{n}}{|x - x_0|^2} = \frac{1}{2\pi} \left(1 + \delta \left[\frac{\sigma \cos(\theta - \theta_0) - \sigma_0 - \sigma' \sin(\theta - \theta_0)}{1 - \cos(\theta - \theta_0)} \right] \right) + \mathcal{O}(\delta^2).$$

The expression in the square brackets above is bounded for $\theta \to \theta_0$. Therefore, (A.2) is uniformly valid for all $\theta \in [0, 2\pi)$. Next, we let $f(\theta)$ denote the term in the square brackets in (A.2) and we expand it in a Fourier series as

(A.3)
$$f(\theta) \equiv \frac{\sigma \cos(\theta - \theta_0) - \sigma_0 - \sigma' \sin(\theta - \theta_0)}{1 - \cos(\theta - \theta_0)}$$
$$= \sum_{m=1}^{\infty} \left[A_m \cos m(\theta - \theta_0) + B_m \sin m(\theta - \theta_0) \right],$$

where A_m and B_m for $m \geq 1$ are defined in terms of integrals I_1 and I_2, which must be calculated, by
(A.4)
$$I_1 \equiv \pi A_m = \int_0^{2\pi} f(\theta) \cos m(\theta - \theta_0) \, d\theta, \qquad I_2 \equiv \pi B_m \int_0^{2\pi} f(\theta) \sin m(\theta - \theta_0) \, d\theta.$$

First, we consider the case where $\sigma = \cos n\theta = \text{Re}\left(e^{in\theta}\right)$. We write I_1 in (A.4) as

$$I_1 = \text{Re} \int_0^{2\pi} \left(\frac{\cos(\theta - \theta_0)e^{in\theta} - e^{in\theta_0} - ine^{in\theta} \sin(\theta - \theta_0)}{1 - \cos(\theta - \theta_0)} \right) \cos m(\theta - \theta_0) \, d\theta.$$

Let $z = e^{i\theta}$, $z_0 = e^{i\theta_0}$, and $w = \frac{z}{z_0}$. Then, $I_1 = \text{Re}(I)$, where I is the following contour integral over the unit disk:

$$I = iz_0^n \int_{|w|=1} G(w) \left(w^m + w^{-m} \right) dw,$$

$$G(w) \equiv \left(\frac{(1 - n)}{2} w^{n+1} + \frac{(1 + n)}{2} w^{n-1} - 1 \right) (1 - w)^{-2}.$$

Since $(1 - w)^2 = \frac{d}{dw} \sum_{n=0}^{\infty} w^n$, then $G(w) = -\left(1 + 2w + 3w^2 + \cdots + (n - 1)w^{n-2} + \frac{(n-1)}{2} w^{n-1} + \cdots \right)$. From the residue theorem we calculate

(A.5)
$$I = z_0^n \begin{cases} 2\pi m, & 1 \leq m < n, \\ \pi(n - 1), & m = n, \\ 0, & m > n, \end{cases}$$

so that $I_1 = \text{Re}(I)$. Similarly, we can obtain I_2 when $\sigma = \cos(n\theta_0)$. In this way, we obtain

$$I_1 = \cos(n\theta_0) \begin{cases} 2\pi m, & 1 \leq m < n, \\ \pi(n-1), & m = n, \\ 0, & m > n, \end{cases} \qquad I_2 = -\sin(n\theta_0) \begin{cases} 2\pi m, & 1 \leq m < n, \\ \pi(n-1), & m = n, \\ 0, & m > n. \end{cases}$$

Alternatively, for $\sigma = \sin(n\theta_0)$, we get

$$I_1 = \sin(n\theta_0) \begin{cases} 2\pi m, & 1 \leq m < n, \\ \pi(n-1), & m = n, \\ 0, & m > n, \end{cases} \qquad I_2 = \cos(n\theta_0) \begin{cases} 2\pi m, & 1 \leq m < n, \\ \pi(n-1), & m = n, \\ 0, & m > n. \end{cases}$$

This determines A_n and B_n as $A_n = \frac{1}{\pi}I_1$ and $B_n = \frac{1}{\pi}I_2$. Therefore, for $\sigma = \cos(n\theta_0)$, (A.3) becomes

$$f(\theta) = (n-1)\left(\cos n\theta_0 \cos n(\theta - \theta_0) - \sin n\theta_0 \sin n(\theta - \theta_0)\right)$$

(A.6a)
$$+ \sum_{m=1}^{n-1} 2m\left[\cos n\theta_0 \cos m(\theta - \theta_0) - \sin n\theta_0 \sin m(\theta - \theta_0)\right].$$

Alternatively, for $\sigma = \sin(n\theta_0)$, (A.3) becomes

$$f(\theta) = (n-1)\left(\cos n\theta_0 \sin n(\theta - \theta_0) + \sin n\theta_0 \cos n(\theta - \theta_0)\right)$$

(A.6b)
$$+ \sum_{m=1}^{n-1} 2m\left[\cos n\theta_0 \sin m(\theta - \theta_0) + \sin n\theta_0 \cos m(\theta - \theta_0)\right].$$

Since $\sigma = \sum_{n=1}^{\infty}(a_n \cos n\theta + b_n \sin n\theta)$ from (4.23), we determine $f(\theta)$ by summing (A.6) over n. We then interchange the order of summation by using $\sum_{n=1}^{\infty}\sum_{m=1}^{n-1}\chi_{mn} = \sum_{m=1}^{\infty}\sum_{n>m}^{\infty}\chi_{mn} = \sum_{n=1}^{\infty}\sum_{m>n}^{\infty}\chi_{nm}$ to obtain

$$f(\theta) = \sum_{n=1}^{\infty}\left(A_n \cos n(\theta - \theta_0) + B_n \sin n(\theta - \theta_0)\right),$$

(A.7) $A_n = (n-1)\left(a_n \cos n\theta_0 + b_n \sin n\theta_0\right) + 2n\sum_{m>n}^{\infty}\left(a_m \cos m\theta_0 + b_m \sin m\theta_0\right),$

$$B_n = (n-1)\left(b_n \cos n\theta_0 - a_n \sin n\theta_0\right) + 2n\sum_{m>n}^{\infty}\left(b_m \cos m\theta_0 - a_m \sin m\theta_0\right).$$

Next, we introduce $S(x; x_0)$ by

(A.8)
$$R(x; x_0) = S(x; x_0) + \frac{|x|^2}{4|\Omega|}.$$

By combining (A.8) and (A.1), we obtain that $S(x; x_0)$ satisfies

(A.9)
$$\triangle S(x; x_0) = 0, \quad x \in \Omega;$$
$$\partial_n S(x; x_0) = \partial_n\left[R(x; x_0) - \frac{|x|^2}{4|\Omega|}\right] \sim \frac{\delta}{2\pi}\left(f(\theta) - \sigma(\theta)\right) + \mathcal{O}(\delta^2), \quad x \in \partial\Omega.$$

In deriving the boundary condition in (A.9) we used (A.2), (A.3), $|\Omega| \approx \pi$, and $\partial_n \left(|x|^2\right) = 2r \left(1 + (r')^2/r^2\right)^{-1/2}$. The $\mathcal{O}(\delta)$ term in the boundary condition for S in (A.9) suggests that we introduce $S_0(x; x_0)$ by

$$(\text{A.10}) \qquad\qquad S(x; x_0) = \frac{\delta}{2\pi} S_0(x; x_0) \,.$$

To leading order we get $\partial_n S_0 = \partial_r S_0|_{r=1} + \mathcal{O}(\delta)$. From (A.9) and (A.10), we obtain that S_0 satisfies

$$(\text{A.11}) \qquad \begin{aligned} \triangle S_0(x; x_0) &= 0\,, & 0 \leq r \leq 1,\ 0 \leq \theta < 2\pi\,; \\ \partial_r S_0(x; x_0)|_{r=1} &= f(\theta) - \sigma(\theta)\,, & r = 1\,. \end{aligned}$$

The solution to (A.11) is written as

$$(\text{A.12}) \qquad S_0 = D_0 + \sum_{n=1}^{\infty} r^n \left[D_n \cos n(\theta - \theta_0) + E_n \sin n(\theta - \theta_0)\right]\,.$$

To determine the coefficients D_n and E_n we must use the boundary condition in (A.11). To this end, we must rewrite σ, given by (4.23), in terms of $\cos n(\theta - \theta_0)$ and $\sin n(\theta - \theta_0)$. This yields
(A.13)
$$\sigma = \sum_{n=1}^{\infty} \left([a_n \cos n\theta_0 + b_n \sin n\theta_0] \cos n(\theta - \theta_0) + [b_n \cos n\theta_0 - a_n \sin n\theta_0] \sin n(\theta - \theta_0)\right)\,.$$

Then, we differentiate (A.12) at $r = 1$ and use (A.7), (A.11), and (A.13) to determine D_n and E_n for $n \geq 1$ as
(A.14)
$$nD_n = A_n - [a_n \cos n\theta_0 + b_n \sin n\theta_0]\,, \qquad nE_n = B_n - [b_n \cos n\theta_0 - a_n \sin n\theta_0]\,.$$

We remark that the constant D_0 in (A.12) can be chosen to ensure that $\int_\Omega G(x; x_0)\, dx = 0$.

In summary, it follows from (A.8) and (A.10) that, for $x \in \partial\Omega$,

$$R(x; x_0) = S(x; x_0) + \frac{|x|^2}{4\pi} = \frac{\delta}{2\pi} S_0(x; x_0) + \frac{1}{4\pi} + \frac{\delta\sigma}{2\pi} + \mathcal{O}(\delta^2)\,, \qquad x \in \partial\Omega\,.$$

By using the definition (4.24) and the reciprocity property of R, we calculate $\rho'(\theta_0)$ as

$$\begin{aligned} \rho'(\theta_0) &= \frac{d}{d\theta_0} R(x_0(\theta_0), x_0(\theta_0)) = 2\frac{d}{d\theta} R(x(\theta), x_0(\theta_0))|_{\theta=\theta_0} \\ &\sim \frac{\delta}{\pi} \left[\frac{d}{d\theta} S_0(x(\theta), x_0(\theta_0))|_{\theta=\theta_0} + \sigma'(\theta_0)\right] + \mathcal{O}(\delta^2)\,. \end{aligned}$$

Then, by using (A.12) and (A.13), we obtain

$$\rho'(\theta_0) = \frac{\delta}{\pi} \sum_{n=1}^{\infty} \left(nE_n + n\left[b_n \cos n\theta_0 - a_n \sin n\theta_0\right]\right)\,.$$

Finally, we use (A.14) to relate D_n to B_n, and then we recall (A.7) for B_n. This yields that

(A.15)

$$\rho'(\theta_0) = \frac{\delta}{\pi} \sum_{n=1}^{\infty} \left(2(n-1)\gamma_n + 2n \sum_{m>n}^{\infty} \gamma_m \right), \qquad \gamma_m = b_m \cos m\theta_0 - a_m \sin m\theta_0 \,.$$

To simplify (A.15) we use the identity $\sum_{n=1}^{\infty} \sum_{m>n}^{\infty} 2n\gamma_m = \sum_{m=2}^{\infty} \gamma_m \sum_{n=1}^{m-1} 2n = \sum_{n=1}^{\infty} n(n-1)\gamma_n$. This yields the final result (4.25) and completes the proof of Principal Result 4.3. ⬜

Acknowledgment. M. J. W. is grateful to Prof. Cyril Muratov of NJIT for exhibiting the connection between our results and the dilute fraction limit of homogenization theory discussed in section 3.

REFERENCES

[1] O. Bénichou and R. Voituriez, *Narrow escape time problem: Time needed for a particle to exit a confining domain through a small window*, Phys. Rev. Lett., 100 (2008), 168105.

[2] P. C. Bressloff, B. A. Earnshaw, and M. J. Ward, *Diffusion of protein receptors on a cylindrical dendritic membrane with partially absorbing traps*, SIAM J. Appl. Math., 68 (2008), pp. 1223–1246.

[3] A. Burchard and J. Denzler, *On the geometry of optimal windows, with special focus on the square*, SIAM J. Math. Anal., 37 (2006), pp. 1800–1827.

[4] N. Chao, S. H. Young, and M. Poo, *Localization of cell membrane components by surface diffusion into a trap*, Biophys. J., 36 (1981), pp. 139–153.

[5] A. F. Cheviakov, M. J. Ward, and R. Straube, *An asymptotic analysis of the mean first passage time for narrow escape problems: Part II: The sphere*, Multiscale Model. Simul., 8 (2010), pp. 836–870.

[6] D. Coombs, R. Straube, and M. Ward, *Diffusion on a sphere with localized traps: Mean first passage time, eigenvalue asymptotics, and Fekete points*, SIAM J. Appl. Math., 70 (2009), pp. 302–332.

[7] A. M. Davis and S. G. Llewellyn Smith, *Perturbation of eigenvalues due to gaps in two-dimensional boundaries*, Proc. R. Soc. Lond. Ser. A Math. Phys. Eng. Sci., 463 (2007), pp. 759–786.

[8] J. Denzler, *Windows of a given area with minimal heat diffusion*, Trans. Amer. Math. Soc., 351 (1999), pp. 569–680.

[9] I. V. Grigoriev, Y. A. Makhnovskii, A. M. Berezhkovskii, and V. Y. Zitserman, *Kinetics of escape through a small hole*, J. Chem. Phys., 116 (2002), pp. 9574–9577.

[10] D. Holcman and Z. Schuss, *Escape through a small opening: Receptor trafficking in a synaptic membrane*, J. Stat. Phys., 117 (2004), pp. 975–1014.

[11] D. Holcman and Z. Schuss, *Diffusion escape through a cluster of small absorbing windows*, J. Phys. A, 41 (2008), 155001.

[12] T. Kolokolnikov, M. Titcombe, and M. J. Ward, *Optimizing the fundamental Neumann eigenvalue for the Laplacian in a domain with small traps*, European J. Appl. Math., 16 (2005), pp. 161–200.

[13] T. Kolokolnikov, M. J. Ward, and J. Wei, *Spot self-replication and dynamics for the Schnakenburg model in a two-dimensional domain*, J. Nonlinear Sci., 19 (2009), pp. 1–56.

[14] C. B. Muratov and S. Y. Shvartsman, *Boundary homogenization for periodic arrays of absorbers*, Multiscale Model. Simul., 7 (2008), pp. 44–61.

[15] S. Redner, *A Guide to First-Passage Time Processes*, Cambridge University Press, Cambridge, UK, 2001.

[16] Z. Schuss, *Theory and Applications of Stochastic Differential Equations*, Wiley Ser. Probab. Stat., John Wiley & Sons, New York, 1980.

[17] Z. Schuss, A. Singer, and D. Holcman, *The narrow escape problem for diffusion in cellular microdomains*, Proc. Natl. Acad. Sci. USA, 104 (2007), pp. 16098–16103.

[18] A. Singer, Z. Schuss, and D. Holcman, *Narrow escape, Part II: The circular disk*, J. Stat. Phys., 122 (2006), pp. 465–489.

[19] A. Singer, Z. Schuss, and D. Holcman, *Narrow escape, Part III: Non-smooth domains and Riemann surfaces*, J. Stat. Phys., 122 (2006), pp. 491–509.

[20] R. Straube, M. J. Ward, and M. Falcke, *Reaction-rate of small diffusing molecules on a cylindrical membrane*, J. Stat. Phys., 129 (2007), pp. 377–405.

[21] A. TAFLIA AND D. HOLCMAN, *Dwell time of a Brownian molecule in a microdomain with traps and a small hole on the boundary*, J. Chem. Phys., 126 (2007), 234107.

[22] M. J. WARD, W. D. HENSHAW, AND J. B. KELLER, *Summing logarithmic expansions for singularly perturbed eigenvalue problems*, SIAM J. Appl. Math., 53 (1993), pp. 799–828.

[23] M. J. WARD AND J. B. KELLER, *Strong localized perturbations of eigenvalue problems*, SIAM J. Appl. Math., 53 (1993), pp. 770–798.

[24] D. WEAVER, *Diffusion-mediated localization on membrane surfaces*, Biophys. J., 41 (1983), pp. 81–86.